Multivalent Amino Sugars to Recognize Different TAR RNA Conformations

Patrick C. Kellish[a], Sunil Kumar[a], Todd S. Mack[c], Meredith Newby Spano[b], Mirko Hennig[c] and Dev P. Arya[a,b*]

[a]Laboratory of Medicinal Chemistry, Department of Chemistry, Clemson University, Clemson, South Carolina 29634, United States
[b]NUBAD, LLC, 900B West Faris Rd., Greenville, SC 29605
[c]Department of Biochemistry and Molecular Biology, Medical University of South Carolina, 70 President St., Charleston, SC 29425
* To whom correspondence should be addressed: Dev P Arya, 461 H.L. Hunter Chemistry Labs, Department of Chemistry, Clemson University, Clemson University, Clemson, South Carolina 29634; Phone: +1-864-656-1106; Fax: +1-864-656-6613; E-mail: dparya@clemson.edu.

Supporting Information

Appendices

S1. Chemical Structures of Neomycin Dimers.

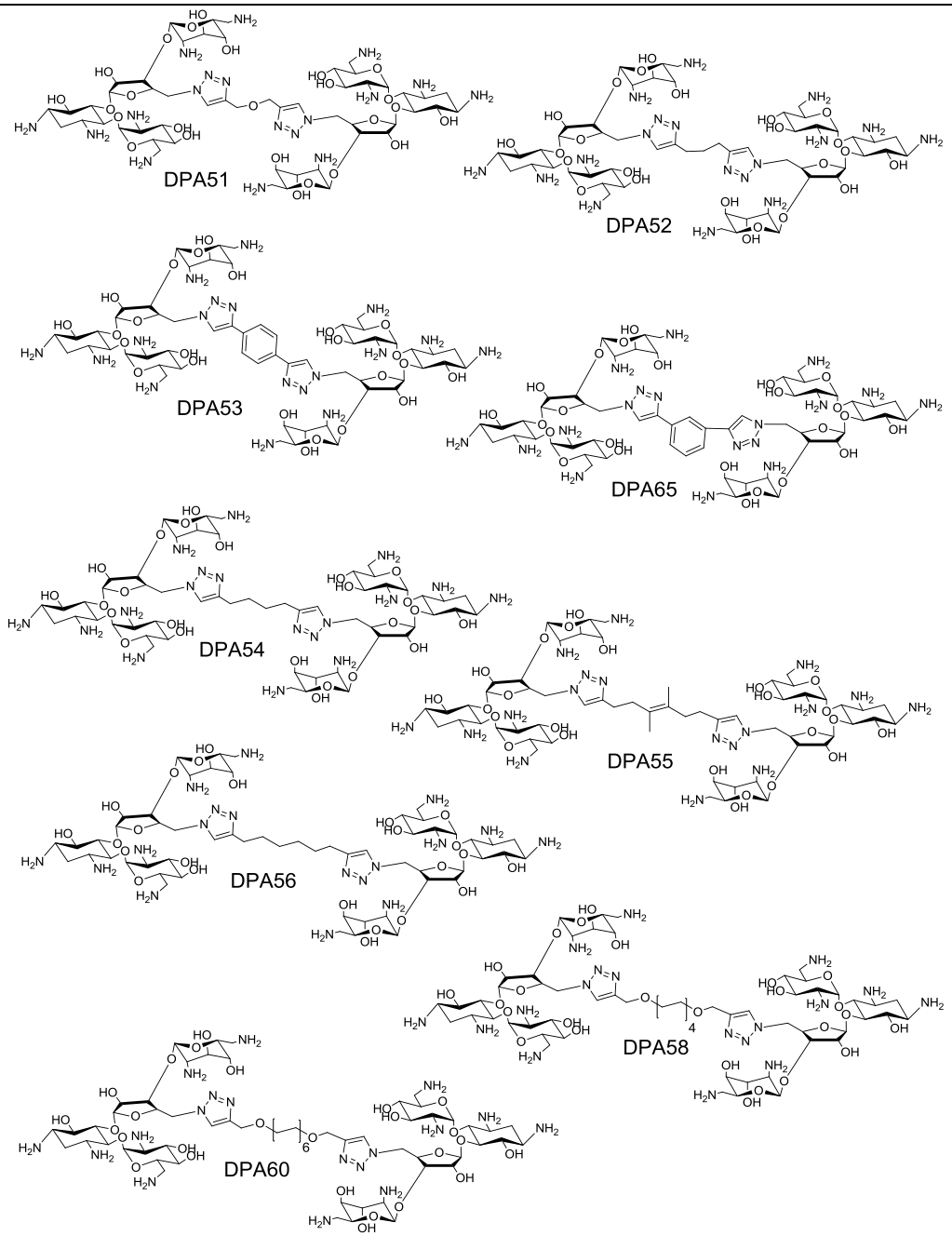

Scheme 1. Chemical structure of neoneo dimers. All the amine groups in neomycin dimers are in salt form (+HCl).

S2. CD Spectroscopy.

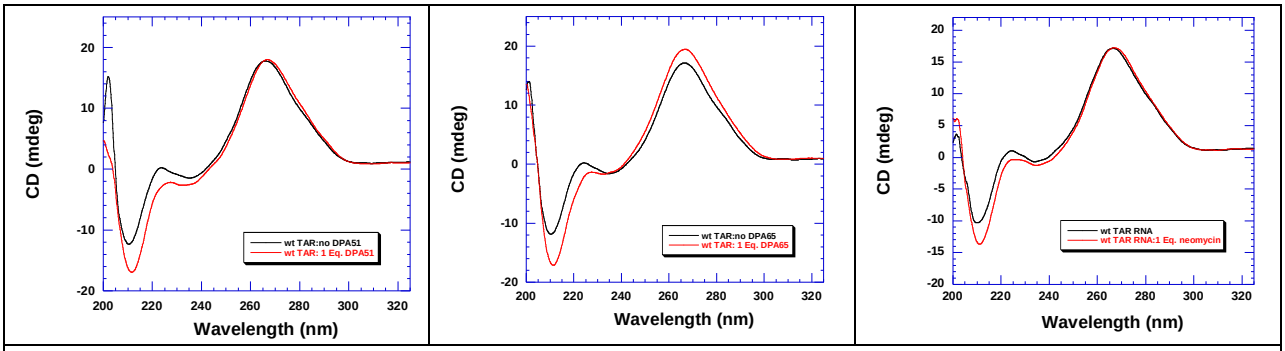

Figure S2.1. CD spectra comparison of wildtype TAR RNA with 1 molar equivalent DPA51 (A), DPA65 (B), and neomycin (C) revealing conformational deviations induced by neomycin dimer or neomycin binding. Buffer conditions: 100 mM KCl, 10 mM SC, 0.5 mM EDTA, pH 6.8. [TAR RNA] = 2µM/strand.

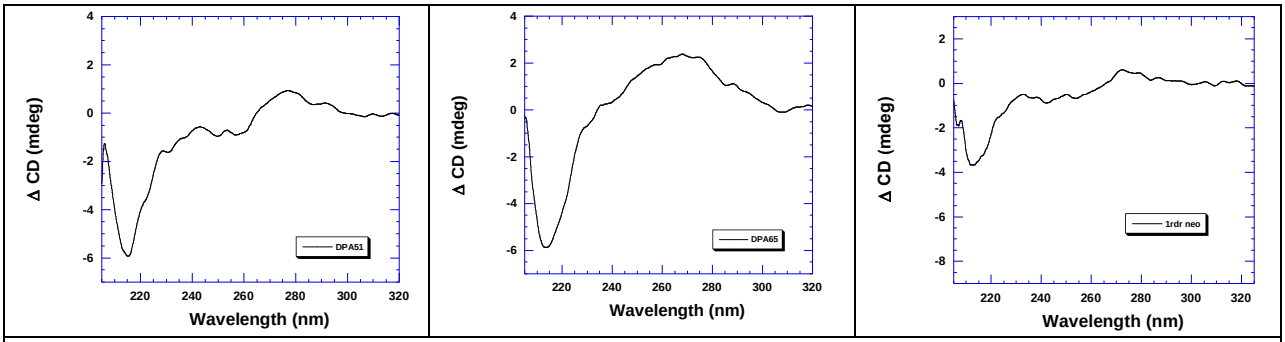

Figure S2.2. Change in wildtype TAR RNA molar ellipticity induced by one molar equivalent DPA51 (A), one molar equivalent DPA65 (B), and neomycin (C). Buffer conditions: 100 mM KCl, 10 mM SC, 0.5 mM EDTA, pH 6.8. [TAR RNA] = 2µM/strand.

S3. UV thermal Denaturation profiles

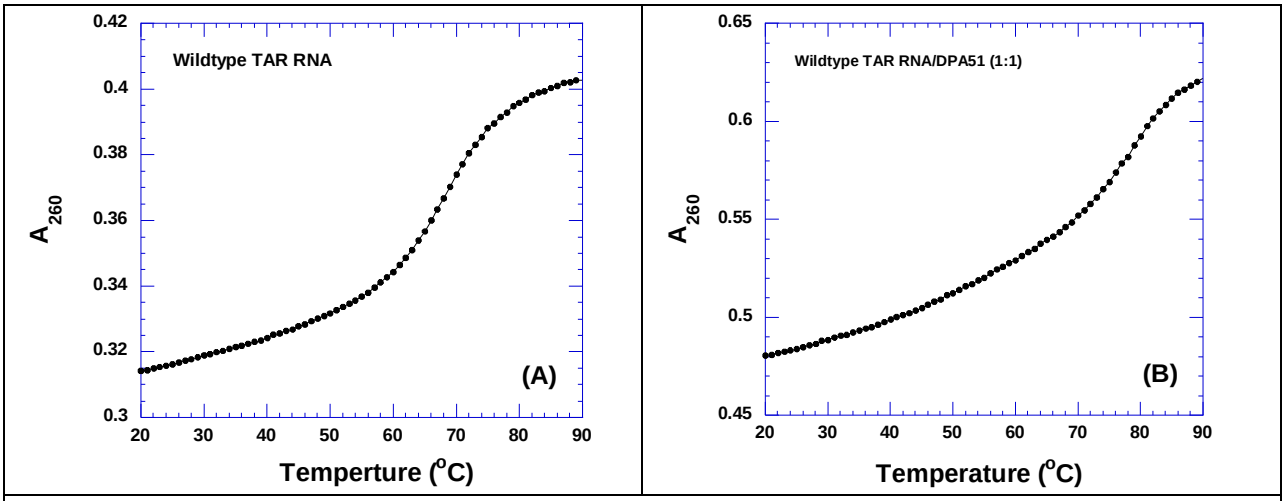

Figure S3.1. UV thermal denaturation profile of wildtype TAR RNA with no drug (A), and with 1 μM (1 mol. eq.) of neomycin dimer DPA51 (B). Buffer conditions: 100 mM KCl, 10 mM SC, 0.5 mM EDTA, pH 6.8. [HIV TAR RNA] = 1 μM/strand. The heating rate was 0.3 °C. Absorbance was recorded at 260nm.

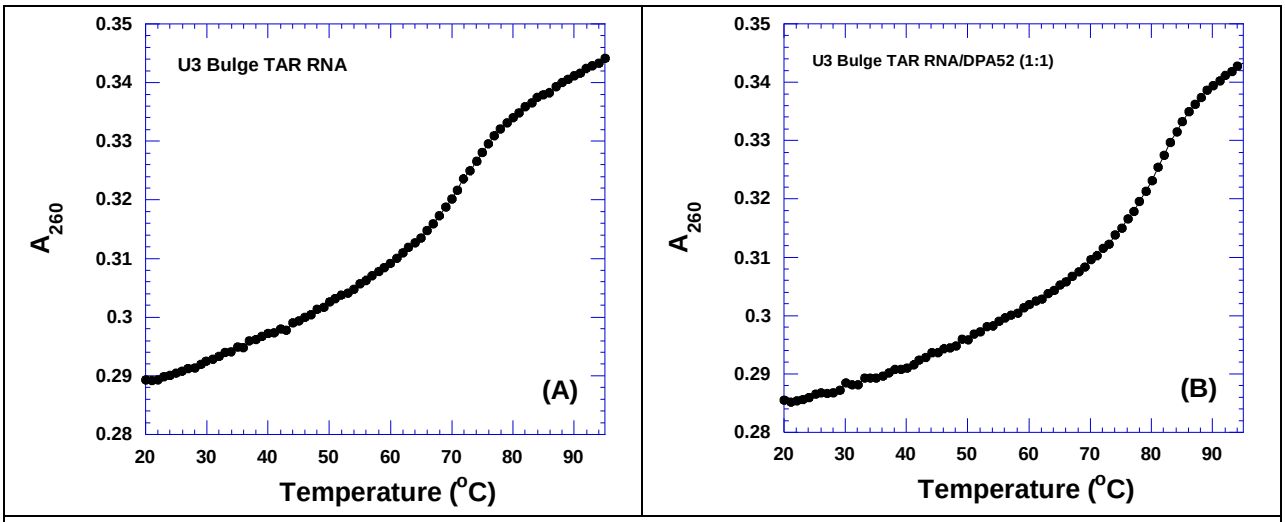

Figure S3.2. UV thermal denaturation profile of the U3 bulge TAR RNA mutant with no drug (A), and with 1 μM (1 mol. eq.) of neomycin dimer DPA51 (B). Buffer conditions: 100 mM KCl, 10 mM SC, 0.5 mM EDTA, pH 6.8. [HIV TAR RNA] = 1 μM/strand. The heating rate was 0.3 °C. Absorbance was recorded at 260nm.

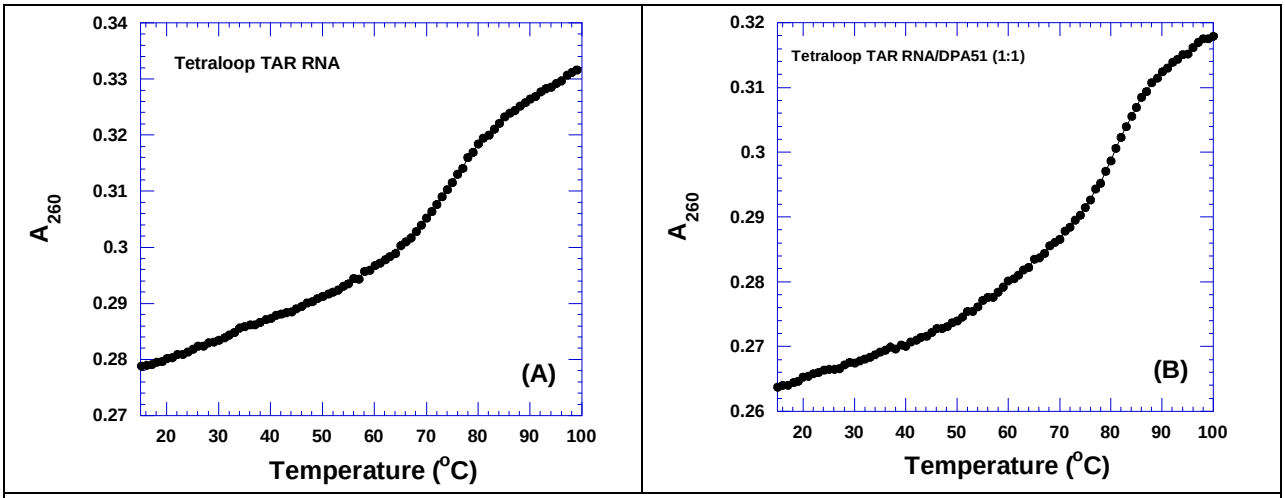

Figure S3.3. UV thermal denaturation profile of the tetraloop TAR RNA mutant with no drug (A), and with 1 μM (1 mol. eq.) of neomycin dimer DPA51 (B). Buffer conditions: 100 mM KCl, 10 mM SC, 0.5 mM EDTA, pH 6.8. [HIV TAR RNA] = 1 μM/strand. The heating rate was 0.3 °C. Absorbance was recorded at 260nm.

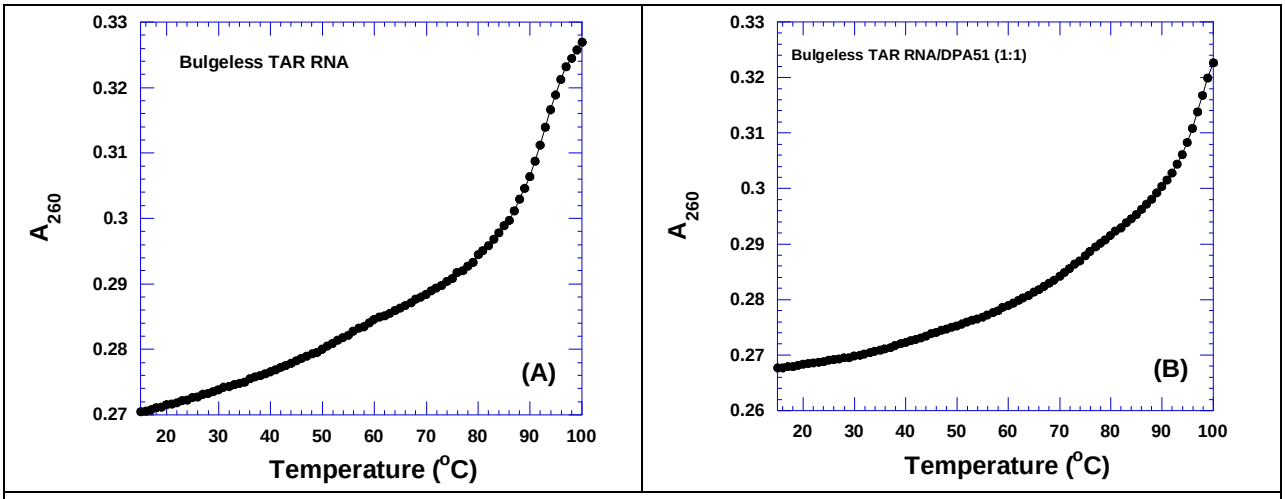

Figure S3.4. UV thermal denaturation profile of the bulgeless TAR RNA mutant with no drug (A), and with 1 μM (1 mol. eq.) of neomycin dimer DPA51 (B). Buffer conditions: 100 mM KCl, 10 mM SC, 0.5 mM EDTA, pH 6.8. [HIV TAR RNA] = 1 μM/strand. The heating rate was 0.3 °C. Absorbance was recorded at 260nm.

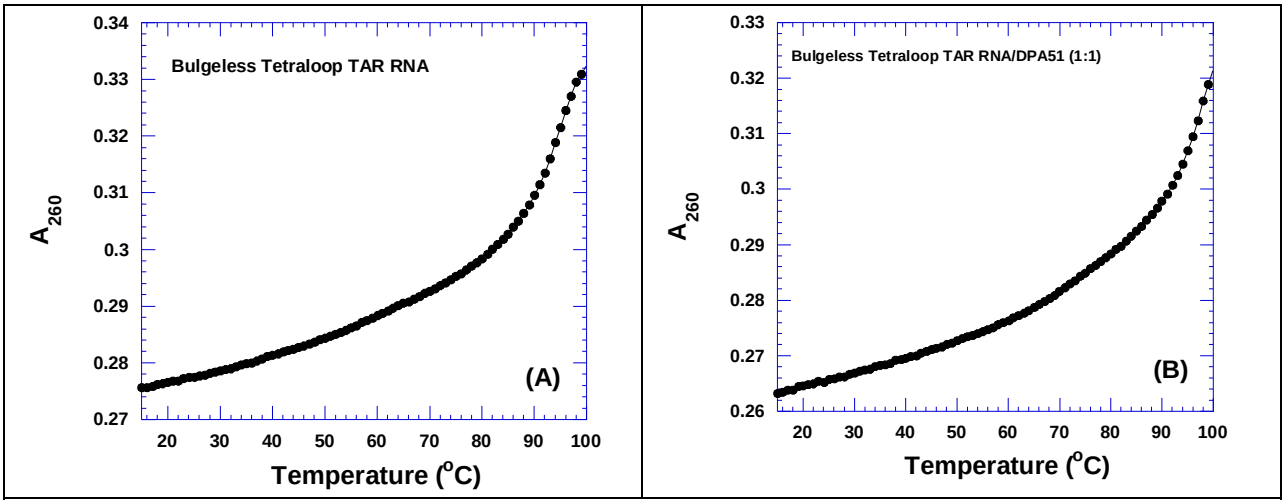

Figure S3.5. UV thermal denaturation profile of the bulgeless tetraloop TAR RNA mutant with no drug (A), and with 1 μM (1 mol. eq.) of neomycin dimer DPA51 (B). Buffer conditions: 100 mM KCl, 10 mM SC, 0.5 mM EDTA, pH 6.8. [HIV TAR RNA] = 1 μM/strand. The heating rate was 0.3 °C. Absorbance was recorded at 260nm.

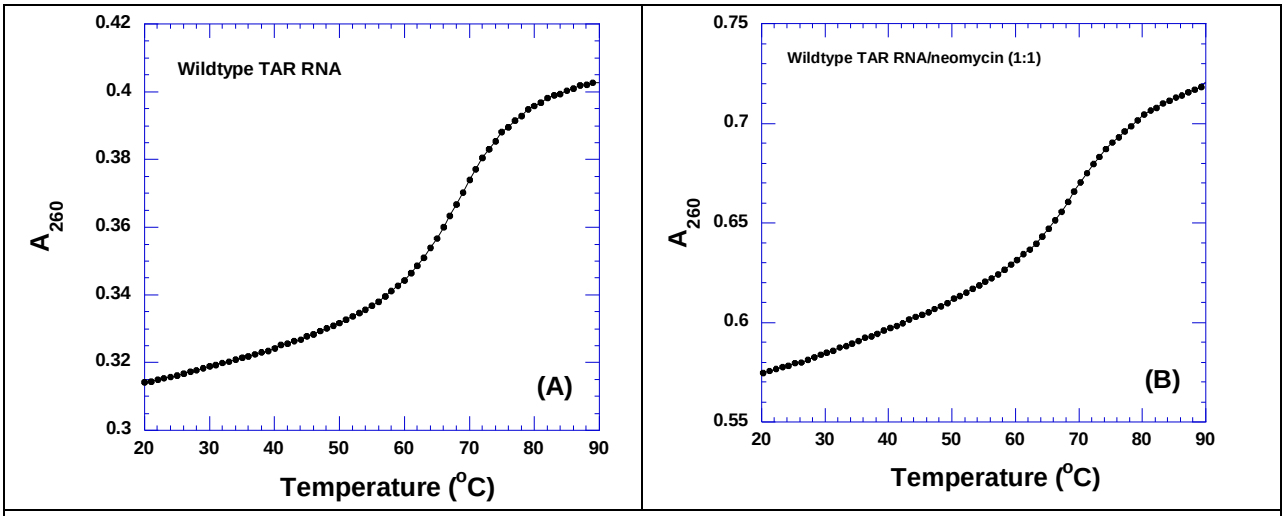

Figure S3.6. UV thermal denaturation profile of wildtype TAR RNA with no drug (A), and with 1 μM (1 mol. eq.) neomycin (B). Buffer conditions: 100 mM KCl, 10 mM SC, 0.5 mM EDTA, pH 6.8. [HIV TAR RNA] = 1 μM/strand. The heating rate was 0.3 °C. Absorbance was recorded at 260nm.

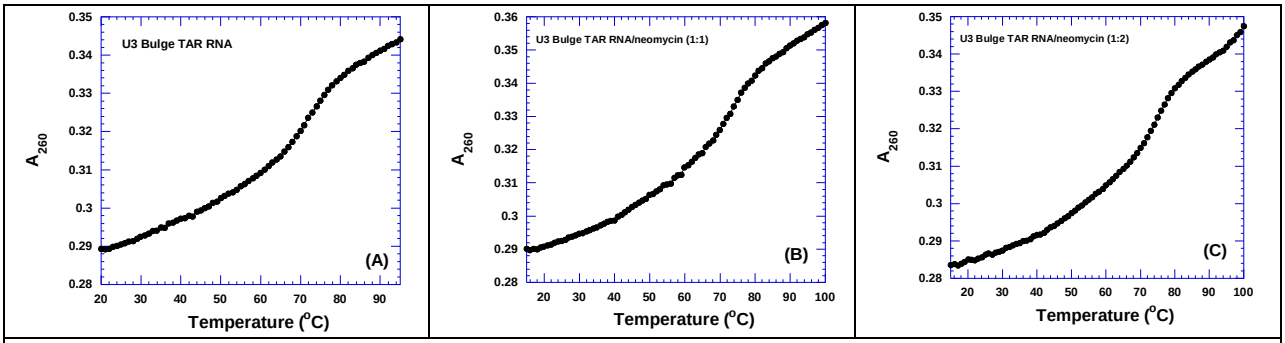

Figure S3.7. UV thermal denaturation profile of the U3 bulge TAR RNA mutant with no drug (A), with 1 μM (1 mol. eq.) neomycin (B), and 2μM (2 mol. Eq.) neomycin (C). Buffer conditions: 100 mM KCl, 10 mM SC, 0.5 mM EDTA, pH 6.8. [HIV TAR RNA] = 1 μM/strand. The heating rate was 0.3 °C. Absorbance was recorded at 260nm.

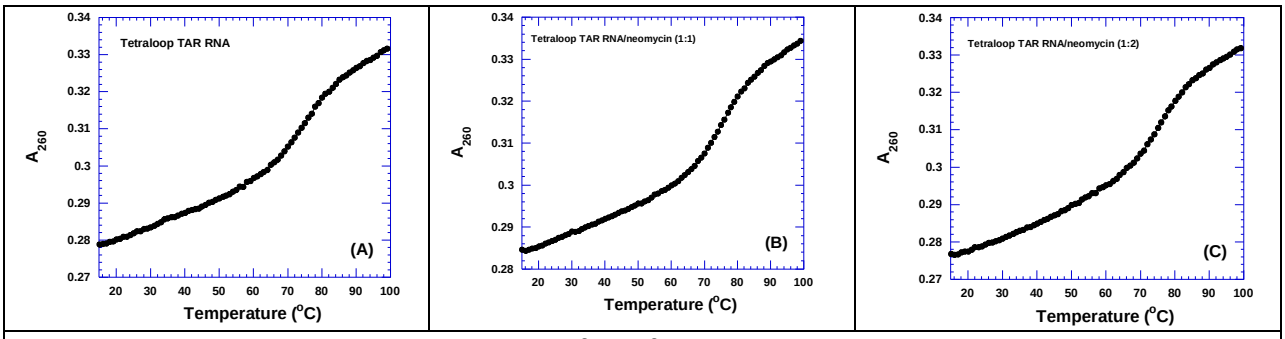

Figure S3.8. UV thermal denaturation profile of the tetraloop TAR RNA mutant with no drug (A), with 1 μM (1 mol. eq.) neomycin (B), and 2μM (2 mol. Eq.) neomycin (C). Buffer conditions: 100 mM KCl, 10 mM SC, 0.5 mM EDTA, pH 6.8. [HIV TAR RNA] = 1 μM/strand. The heating rate was 0.3 °C. Absorbance was recorded at 260nm.

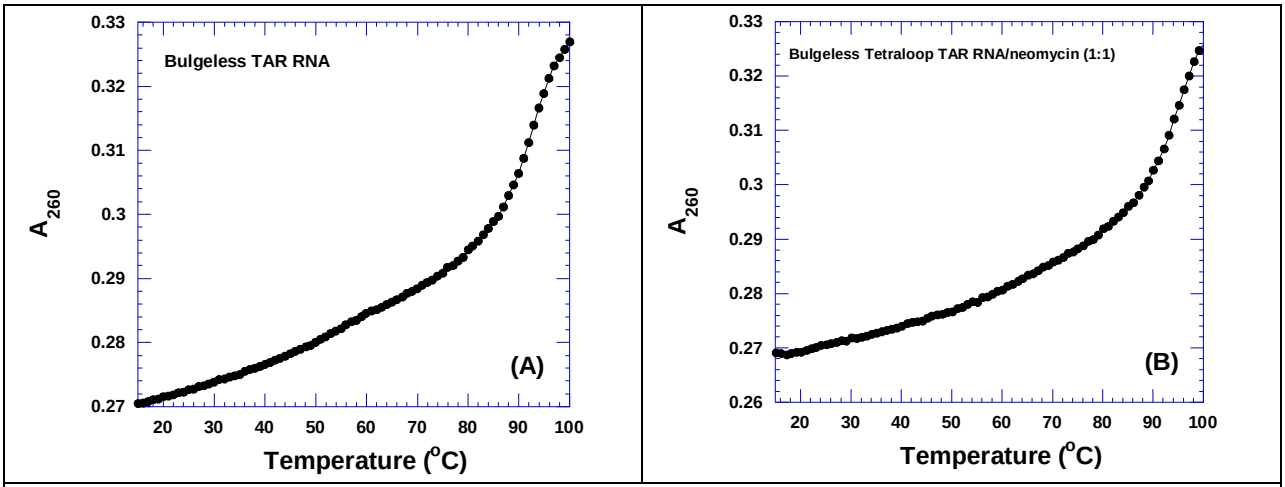

Figure S3.9. UV thermal denaturation profile of the bulgeless TAR RNA mutant with no drug (A), and with 1 μM (1 mol. eq.) neomycin (B). Buffer conditions: 100 mM KCl, 10 mM SC, 0.5 mM EDTA, pH 6.8. [HIV TAR RNA] = 1 μM/strand. The heating rate was 0.3 °C. Absorbance was recorded at 260nm.

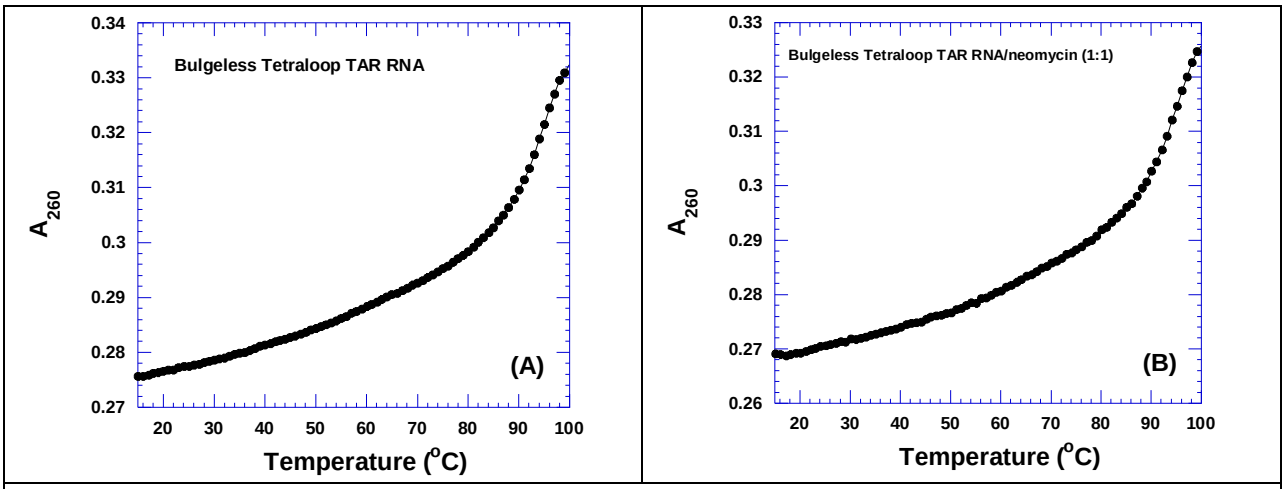

Figure S3.10. UV thermal denaturation profile of the bulgeless tetraloop TAR RNA mutant with no drug (A), and with 1 μM (1 mol. eq.) neomycin (B). Buffer conditions: 100 mM KCl, 10 mM SC, 0.5 mM EDTA, pH 6.8. [HIV TAR RNA] = 1 μM/strand. The heating rate was 0.3 °C. Absorbance was recorded at 260nm.

S4. Mutant TAR RNA Ethidium Bromide Displacement Assays.

The IC_{50} plots shown use concentrations expressed as r_{dr} (ratio of drug to RNA). All ethidium bromide displacement assays used the same 200 nM/strand RNA concentration, therefore the IC_{50} values can be converted from r_{dr} to nM by multiplying the r_{dr} by the RNA concentration used (200 nM/strand).

IC_{50} (nM) = [Ratio of drug to RNA] x [RNA Concentration]

IC_{50} (nM) = r_{dr} x 200 nM/strand

Bulgeless TAR RNA Mutant Ethidium Bromide Displacement Binding Assay

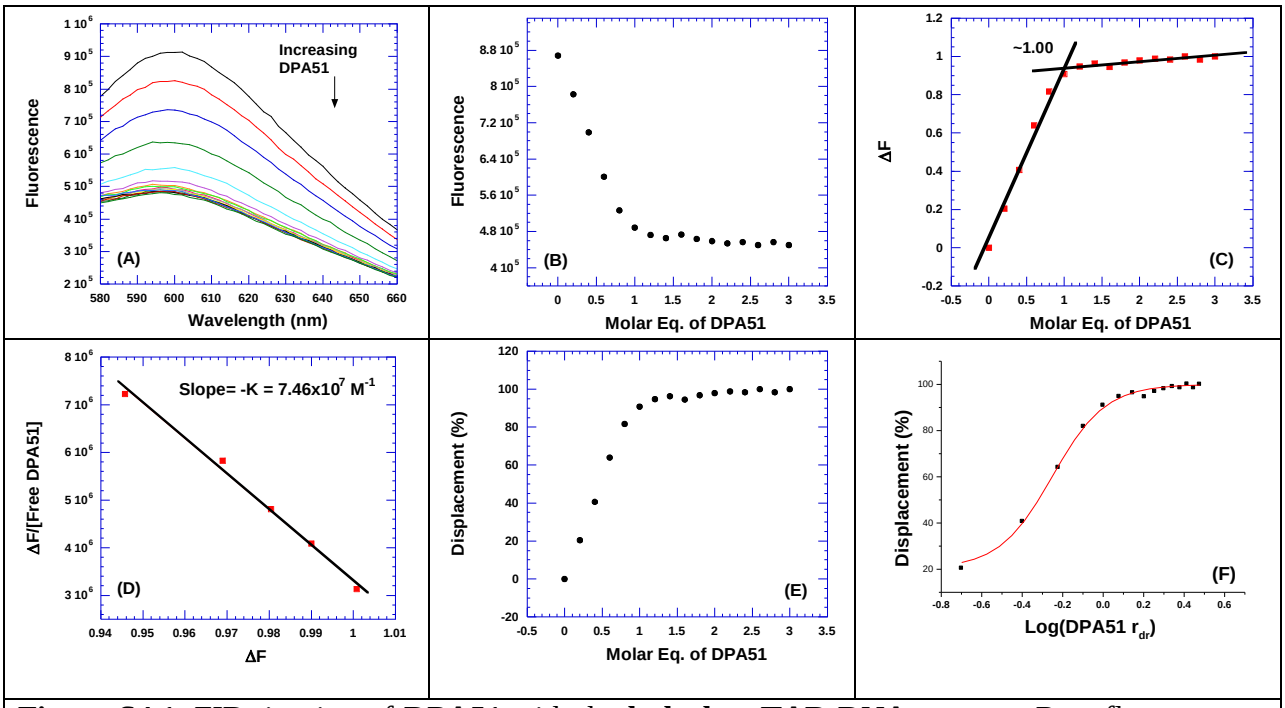

Figure S4.1. FID titration of **DPA51** with the **bulgeless TAR RNA mutant**. Raw fluorescence emission spectra in the presence of increasing concentration of **DPA51** (A). The decrease of fluorescence intensity (at 610 nm) of the bulgeless TAR RNA mutant/EtBr complex with increasing concentration of **DPA51** results in a saturating binding plot (B). The plot between normalized fluorescence intensity (at 610 nm) of the bulgeless TAR RNA mutant-EtBr complex as a function of concentration of **DPA51** results in a saturating binding plot (C). The Scatchard plot analysis of **DPA51** with the bulgeless TAR RNA mutant (D). The plot between normalized EtBr displacement (at 610 nm) of the bulgeless TAR RNA mutant-EtBr complex as a function of concentration of **DPA51** (E). The plot for EtBr displacement (%) of the bulgeless TAR RNA mutant-EtBr complex versus the log of the **DPA51** r_{dr}, the data shown with a sigmoidal fit, was used to determine the IC_{50} value (F). Buffer conditions: 100 mM KCl, 10 mM SC, 0.5 mM EDTA, pH 6.8. Bulgeless TAR RNA mutant = 200 nM/strand. [EtBr] = 5 µM.

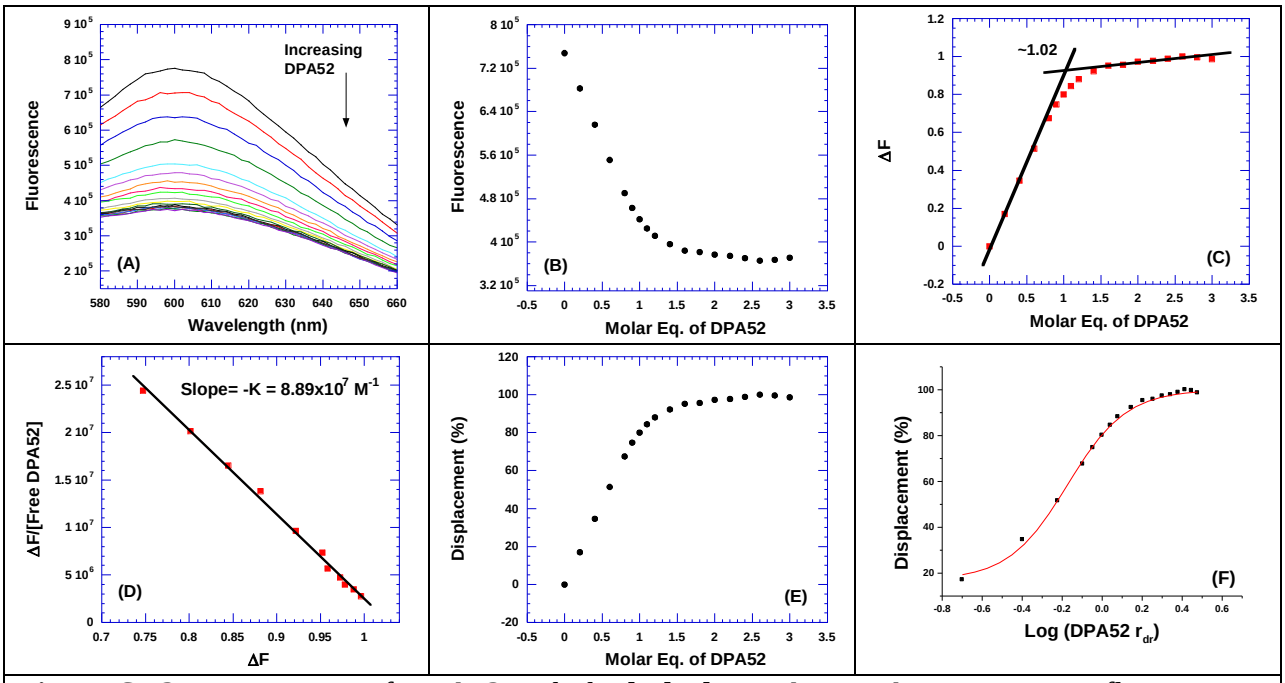

Figure S4.2. FID titration of **DPA52** with the **bulgeless TAR RNA mutant**. Raw fluorescence emission spectra in the presence of increasing concentration of **DPA52** (A). The decrease of fluorescence intensity (at 610 nm) of the bulgeless TAR RNA mutant/EtBr complex with increasing concentration of **DPA52** results in a saturating binding plot (B). The plot between normalized fluorescence intensity (at 610 nm) of the bulgeless TAR RNA mutant-EtBr complex as a function of concentration of **DPA52** results in a saturating binding plot (C). The Scatchard plot analysis of **DPA52** with the bulgeless TAR RNA mutant (D). The plot between normalized EtBr displacement (at 610 nm) of the bulgeless TAR RNA mutant-EtBr complex as a function of concentration of **DPA52** (E). The plot for EtBr displacement (%) of the bulgeless TAR RNA mutant-EtBr complex versus the log of the **DPA52** r_{dr}, the data shown with a sigmoidal fit, was used to determine the IC_{50} value (F). Buffer conditions: 100 mM KCl, 10 mM SC, 0.5 mM EDTA, pH 6.8. Bulgeless TAR RNA mutant = 200 nM/strand. [EtBr] = 5 µM.

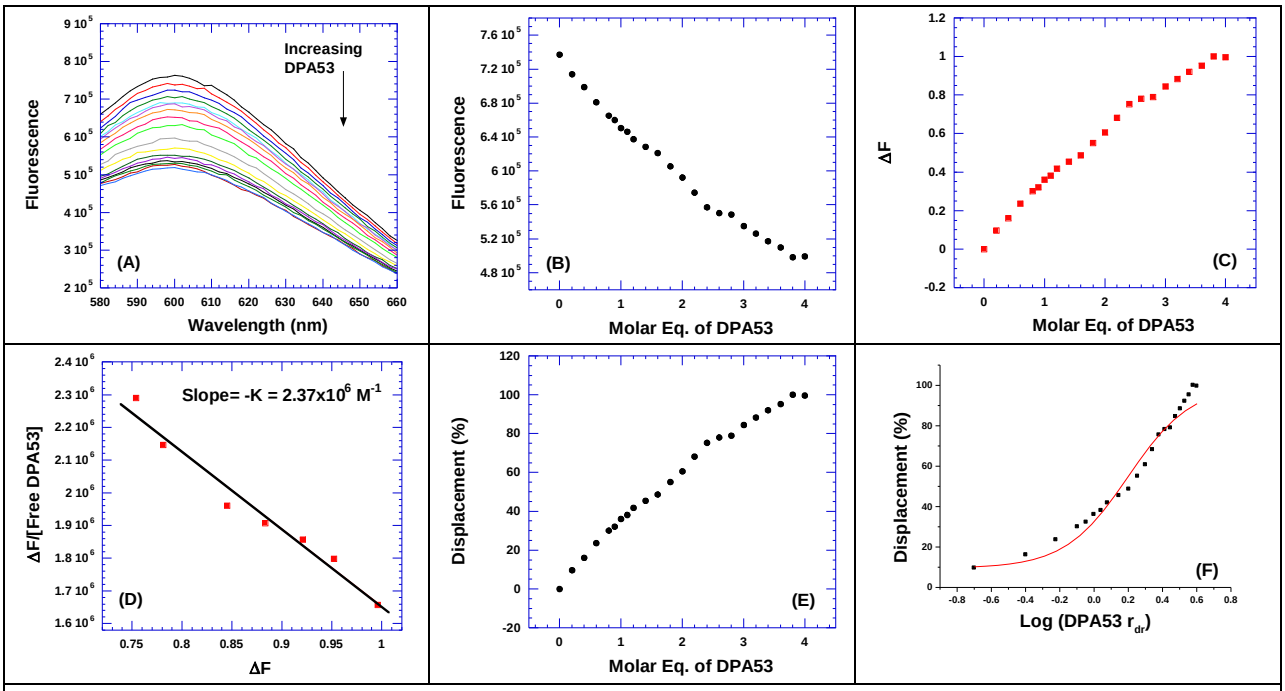

Figure S4.3. FID titration of **DPA53** with the **bulgeless TAR RNA mutant**. Raw fluorescence emission spectra in the presence of increasing concentration of **DPA53** (A). The decrease of fluorescence intensity (at 610 nm) of the bulgeless TAR RNA mutant/EtBr complex with increasing concentration of **DPA53** results in a saturating binding plot (B). The plot between normalized fluorescence intensity (at 610 nm) of the bulgeless TAR RNA mutant-EtBr complex as a function of concentration of **DPA53** results in a saturating binding plot (C). The Scatchard plot analysis of **DPA53** with the bulgeless TAR RNA mutant (D). The plot between normalized EtBr displacement (at 610 nm) of the bulgeless TAR RNA mutant-EtBr complex as a function of concentration of **DPA53** (E). The plot for EtBr displacement (%) of the bulgeless TAR RNA mutant-EtBr complex versus the log of the **DPA53** r_{dr}, the data shown with a sigmoidal fit, was used to determine the IC_{50} value (F). Buffer conditions: 100 mM KCl, 10 mM SC, 0.5 mM EDTA, pH 6.8. Bulgeless TAR RNA mutant = 200 nM/strand. [EtBr] = 5 µM.

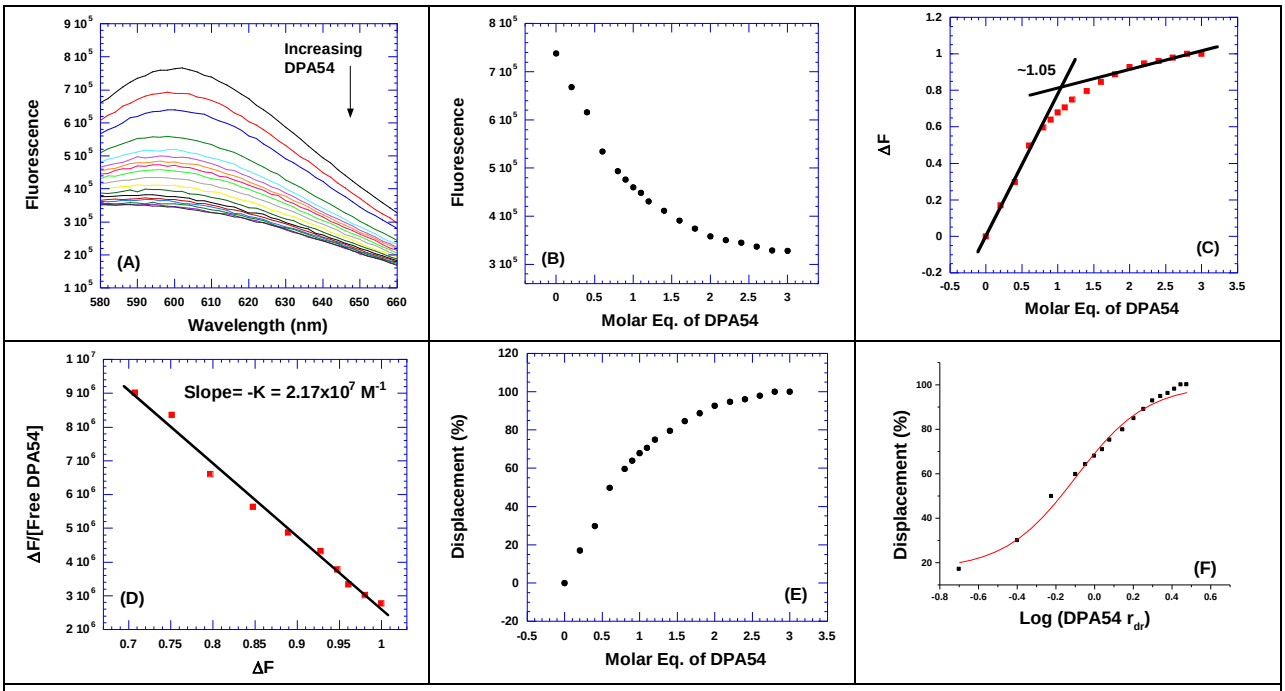

Figure S4.4. FID titration of **DPA54** with the **bulgeless TAR RNA mutant**. Raw fluorescence emission spectra in the presence of increasing concentration of **DPA54** (A). The decrease of fluorescence intensity (at 610 nm) of the bulgeless TAR RNA mutant/EtBr complex with increasing concentration of **DPA54** results in a saturating binding plot (B). The plot between normalized fluorescence intensity (at 610 nm) of the bulgeless TAR RNA mutant-EtBr complex as a function of concentration of **DPA54** results in a saturating binding plot (C). The Scatchard plot analysis of **DPA54** with the bulgeless TAR RNA mutant (D). The plot between normalized EtBr displacement (at 610 nm) of the bulgeless TAR RNA mutant-EtBr complex as a function of concentration of **DPA54** (E). The plot for EtBr displacement (%) of the bulgeless TAR RNA mutant-EtBr complex versus the log of the **DPA54** r_{dr}, the data shown with a sigmoidal fit, was used to determine the IC_{50} value (F). Buffer conditions: 100 mM KCl, 10 mM SC, 0.5 mM EDTA, pH 6.8. Bulgeless TAR RNA mutant = 200 nM/strand. [EtBr] = 5 µM.

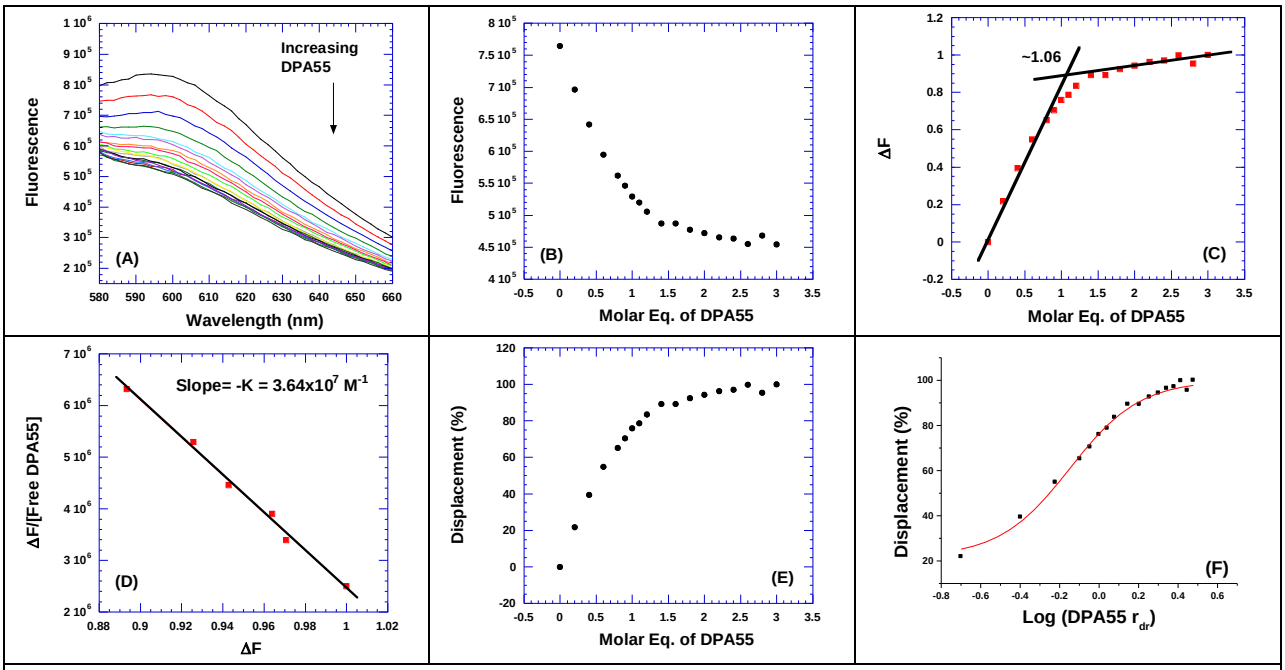

Figure S4.5. FID titration of **DPA55** with the **bulgeless TAR RNA mutant**. Raw fluorescence emission spectra in the presence of increasing concentration of **DPA55** (A). The decrease of fluorescence intensity (at 610 nm) of the bulgeless TAR RNA mutant/EtBr complex with increasing concentration of **DPA55** results in a saturating binding plot (B). The plot between normalized fluorescence intensity (at 610 nm) of the bulgeless TAR RNA mutant-EtBr complex as a function of concentration of **DPA55** results in a saturating binding plot (C). The Scatchard plot analysis of **DPA55** with the bulgeless TAR RNA mutant (D). The plot between normalized EtBr displacement (at 610 nm) of the bulgeless TAR RNA mutant-EtBr complex as a function of concentration of **DPA55** (E). The plot for EtBr displacement (%) of the bulgeless TAR RNA mutant-EtBr complex versus the log of the **DPA55** r_{dr}, the data shown with a sigmoidal fit, was used to determine the IC_{50} value (F). Buffer conditions: 100 mM KCl, 10 mM SC, 0.5 mM EDTA, pH 6.8. Bulgeless TAR RNA mutant = 200 nM/strand. [EtBr] = 5 µM.

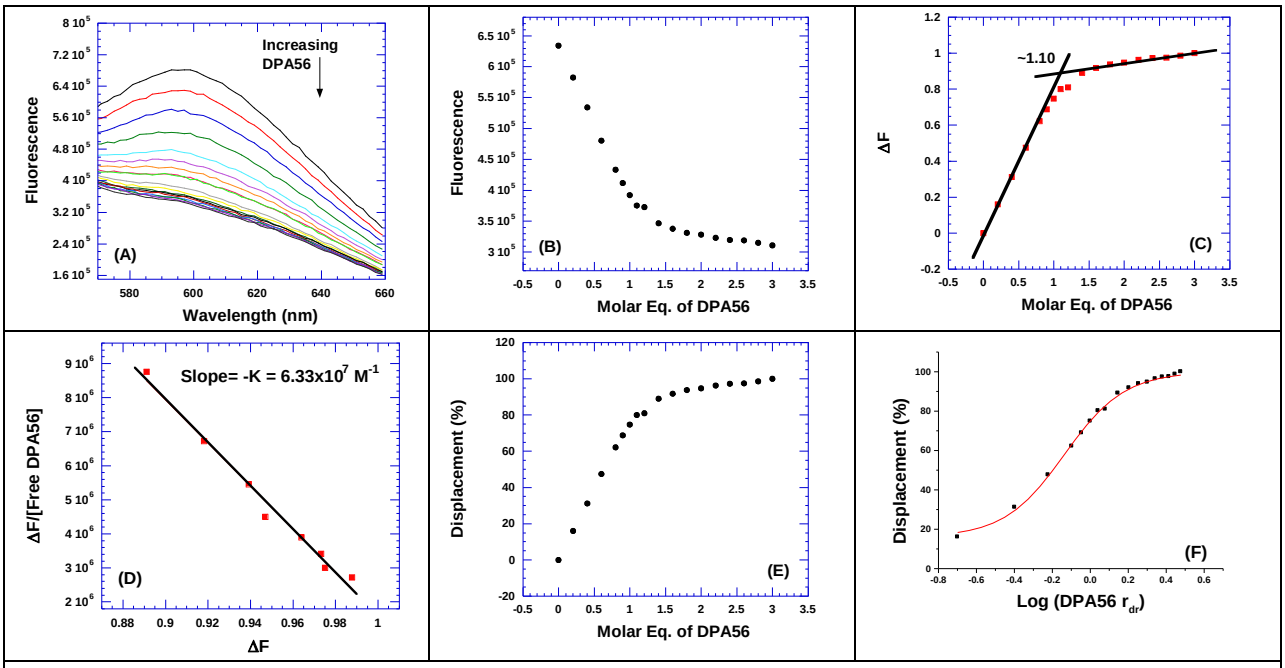

Figure S4.6. FID titration of **DPA56** with the **bulgeless TAR RNA mutant**. Raw fluorescence emission spectra in the presence of increasing concentration of **DPA56** (A). The decrease of fluorescence intensity (at 610 nm) of the bulgeless TAR RNA mutant/EtBr complex with increasing concentration of **DPA56** results in a saturating binding plot (B). The plot between normalized fluorescence intensity (at 610 nm) of the bulgeless TAR RNA mutant-EtBr complex as a function of concentration of **DPA56** results in a saturating binding plot (C). The Scatchard plot analysis of **DPA56** with the bulgeless TAR RNA mutant (D). The plot between normalized EtBr displacement (at 610 nm) of the bulgeless TAR RNA mutant-EtBr complex as a function of concentration of **DPA56** (E). The plot for EtBr displacement (%) of the bulgeless TAR RNA mutant-EtBr complex versus the log of the **DPA56** r_{dr}, the data shown with a sigmoidal fit, was used to determine the IC_{50} value (F). Buffer conditions: 100 mM KCl, 10 mM SC, 0.5 mM EDTA, pH 6.8. Bulgeless TAR RNA mutant = 200 nM/strand. [EtBr] = 5 µM.

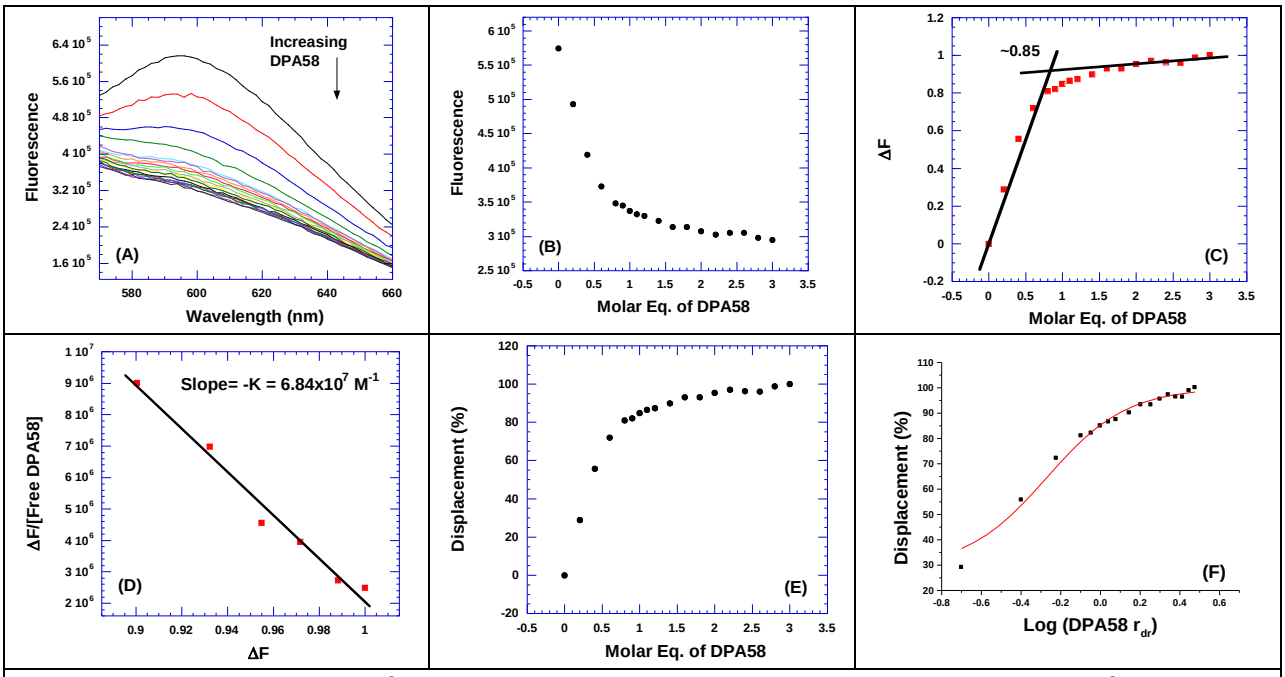

Figure S4.7. FID titration of **DPA58** with the **bulgeless TAR RNA mutant**. Raw fluorescence emission spectra in the presence of increasing concentration of **DPA58** (A). The decrease of fluorescence intensity (at 610 nm) of the bulgeless TAR RNA mutant/EtBr complex with increasing concentration of **DPA58** results in a saturating binding plot (B). The plot between normalized fluorescence intensity (at 610 nm) of the bulgeless TAR RNA mutant-EtBr complex as a function of concentration of **DPA58** results in a saturating binding plot (C). The Scatchard plot analysis of **DPA58** with the bulgeless TAR RNA mutant (D). The plot between normalized EtBr displacement (at 610 nm) of the bulgeless TAR RNA mutant-EtBr complex as a function of concentration of **DPA58** (E). The plot for EtBr displacement (%) of the bulgeless TAR RNA mutant-EtBr complex versus the log of the **DPA58** r_{dr}, the data shown with a sigmoidal fit, was used to determine the IC_{50} value (F). Buffer conditions: 100 mM KCl, 10 mM SC, 0.5 mM EDTA, pH 6.8. Bulgeless TAR RNA mutant = 200 nM/strand. [EtBr] = 5 µM.

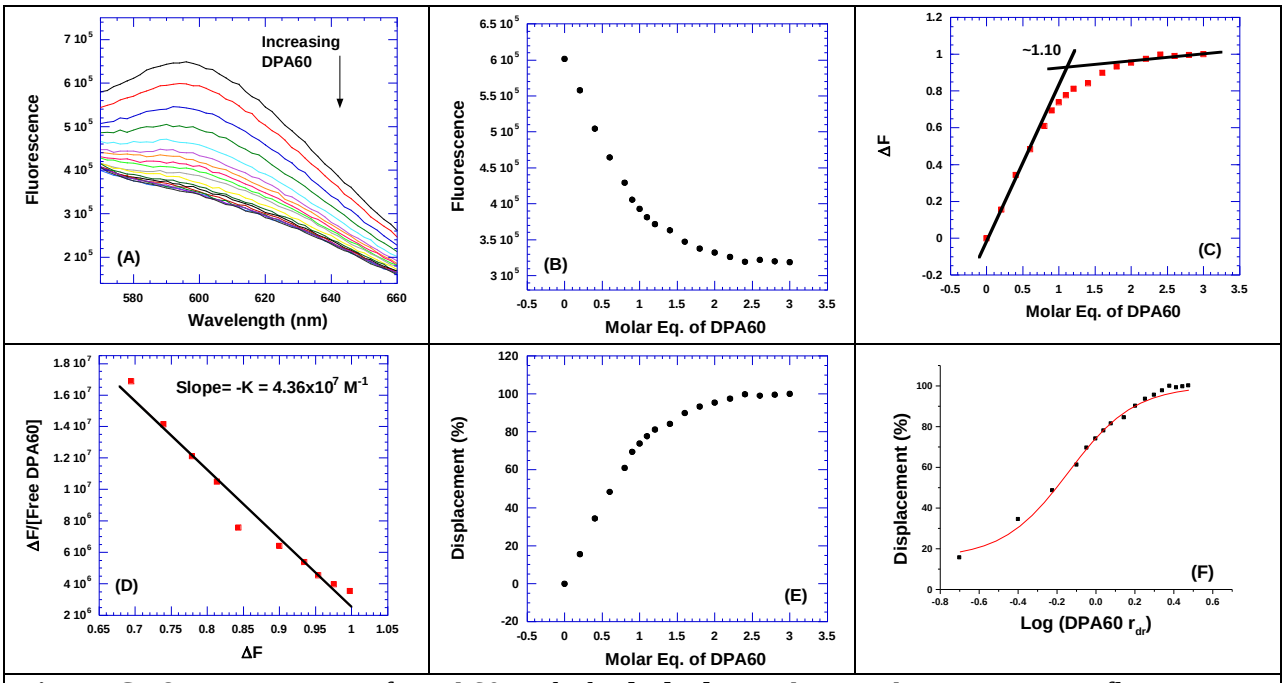

Figure S4.8. FID titration of **DPA60** with the **bulgeless TAR RNA mutant**. Raw fluorescence emission spectra in the presence of increasing concentration of **DPA60** (A). The decrease of fluorescence intensity (at 610 nm) of the bulgeless TAR RNA mutant/EtBr complex with increasing concentration of **DPA60** results in a saturating binding plot (B). The plot between normalized fluorescence intensity (at 610 nm) of the bulgeless TAR RNA mutant-EtBr complex as a function of concentration of **DPA60** results in a saturating binding plot (C). The Scatchard plot analysis of **DPA60** with the bulgeless TAR RNA mutant (D). The plot between normalized EtBr displacement (at 610 nm) of the bulgeless TAR RNA mutant-EtBr complex as a function of concentration of **DPA60** (E). The plot for EtBr displacement (%) of the bulgeless TAR RNA mutant-EtBr complex versus the log of the **DPA60** r_{dr}, the data shown with a sigmoidal fit, was used to determine the IC_{50} value (F). Buffer conditions: 100 mM KCl, 10 mM SC, 0.5 mM EDTA, pH 6.8. Bulgeless TAR RNA mutant = 200 nM/strand. [EtBr] = 5 µM.

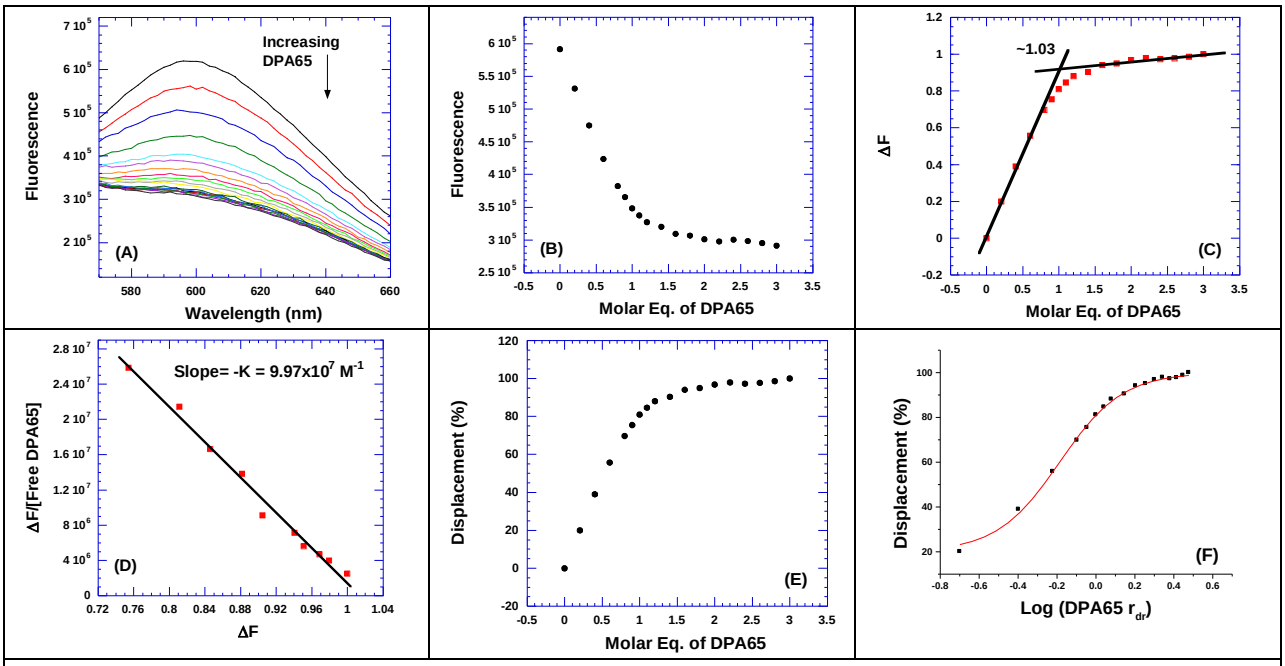

Figure S4.9. FID titration of **DPA65** with the **bulgeless TAR RNA mutant**. Raw fluorescence emission spectra in the presence of increasing concentration of **DPA65** (A). The decrease of fluorescence intensity (at 610 nm) of the bulgeless TAR RNA mutant/EtBr complex with increasing concentration of **DPA65** results in a saturating binding plot (B). The plot between normalized fluorescence intensity (at 610 nm) of the bulgeless TAR RNA mutant-EtBr complex as a function of concentration of **DPA65** results in a saturating binding plot (C). The Scatchard plot analysis of **DPA65** with the bulgeless TAR RNA mutant (D). The plot between normalized EtBr displacement (at 610 nm) of the bulgeless TAR RNA mutant-EtBr complex as a function of concentration of **DPA65** (E). The plot for EtBr displacement (%) of the bulgeless TAR RNA mutant-EtBr complex versus the log of the **DPA65** r_{dr}, the data shown with a sigmoidal fit, was used to determine the IC_{50} value (F). Buffer conditions: 100 mM KCl, 10 mM SC, 0.5 mM EDTA, pH 6.8. Bulgeless TAR RNA mutant = 200 nM/strand. [EtBr] = 5 µM.

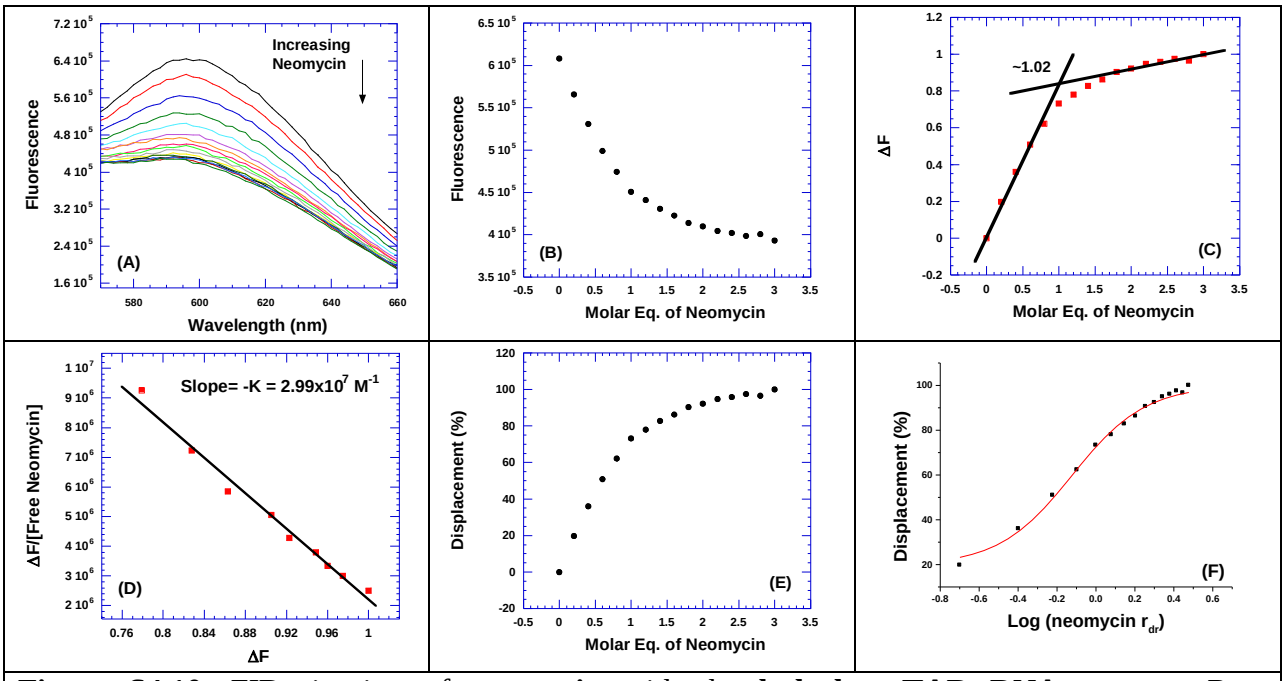

Figure S4.10. FID titration of **neomycin** with the **bulgeless TAR RNA mutant**. Raw fluorescence emission spectra in the presence of increasing concentration of **neomycin** (A). The decrease of fluorescence intensity (at 610 nm) of the bulgeless TAR RNA mutant/EtBr complex with increasing concentration of **neomycin** results in a saturating binding plot (B). The plot between normalized fluorescence intensity (at 610 nm) of the bulgeless TAR RNA mutant-EtBr complex as a function of concentration of **neomycin** results in a saturating binding plot (C). The Scatchard plot analysis of **neomycin** with the bulgeless TAR RNA mutant (D). The plot between normalized EtBr displacement (at 610 nm) of the bulgeless TAR RNA mutant-EtBr complex as a function of concentration of **neomycin** (E). The plot for EtBr displacement (%) of the bulgeless TAR RNA mutant-EtBr complex versus the log of the **neomycin** r_{dr}, the data shown with a sigmoidal fit, was used to determine the IC_{50} value (F). Buffer conditions: 100 mM KCl, 10 mM SC, 0.5 mM EDTA, pH 6.8. Bulgeless TAR RNA mutant = 200 nM/strand. [EtBr] = 5 µM.

Tetraloop TAR RNA Mutant Ethidium Bromide Displacement Binding Assay

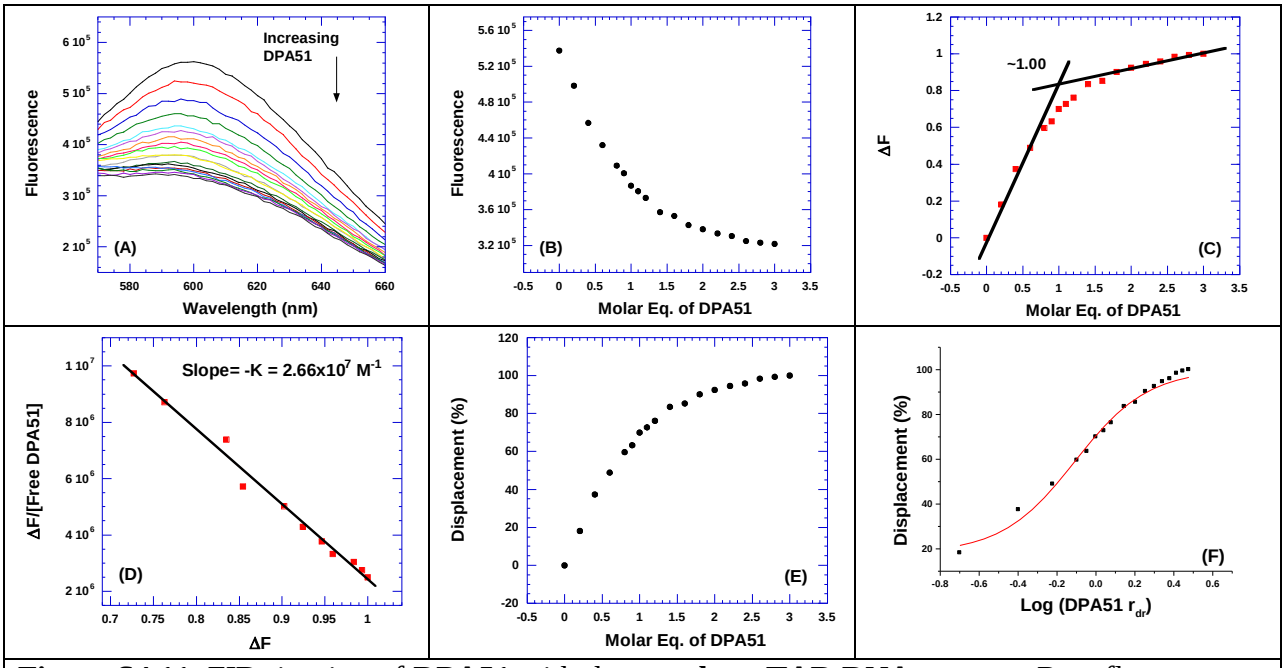

Figure S4.11. FID titration of **DPA51** with the **tetraloop TAR RNA mutant**. Raw fluorescence emission spectra in the presence of increasing concentration of **DPA51** (A). The decrease of fluorescence intensity (at 610 nm) of the tetraloop TAR RNA mutant/EtBr complex with increasing concentration of **DPA51** results in a saturating binding plot (B). The plot between normalized fluorescence intensity (at 610 nm) of the tetraloop TAR RNA mutant-EtBr complex as a function of concentration of **DPA51** results in a saturating binding plot (C). The Scatchard plot analysis of **DPA51** with the tetraloop TAR RNA mutant (D). The plot between normalized EtBr displacement (at 610 nm) of the tetraloop TAR RNA mutant-EtBr complex as a function of concentration of **DPA51** (E). The plot for EtBr displacement (%) of the tetraloop TAR RNA mutant-EtBr complex versus the log of the **DPA51** r_{dr}, the data shown with a sigmoidal fit, was used to determine the IC_{50} value (F). Buffer conditions: 100 mM KCl, 10 mM SC, 0.5 mM EDTA, pH 6.8. Tetraloop TAR RNA mutant = 200 nM/strand. [EtBr] = 5 µM.

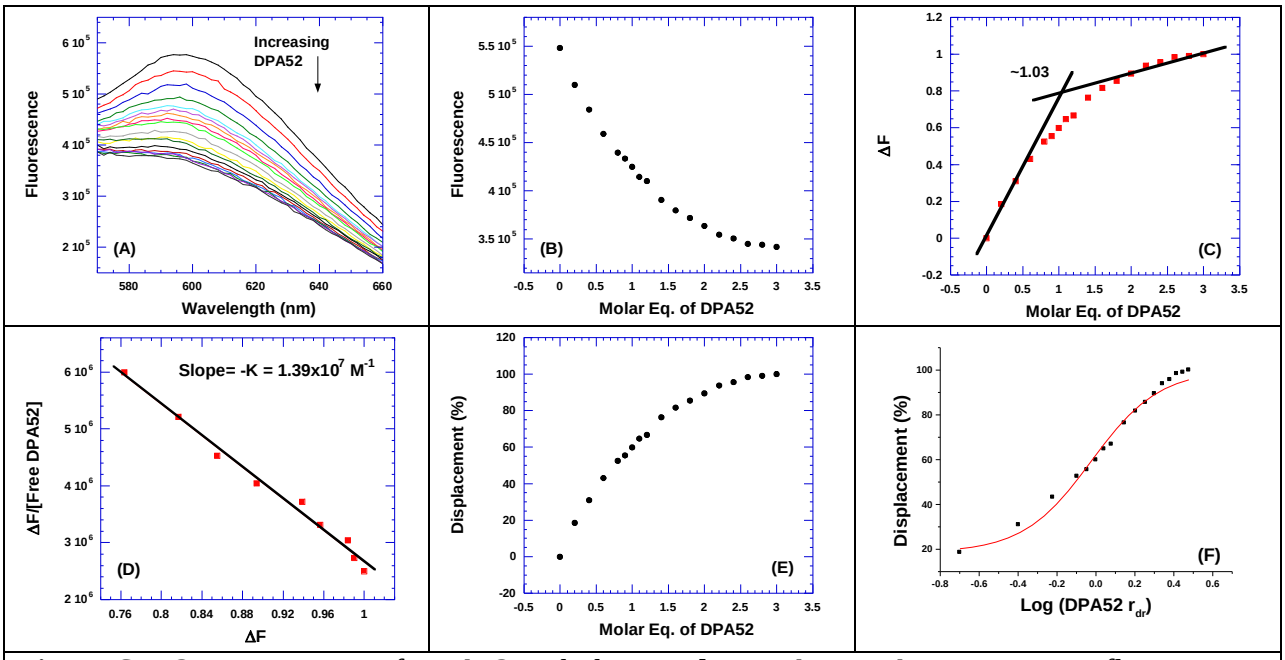

Figure S4.12. FID titration of **DPA52** with the **tetraloop TAR RNA mutant**. Raw fluorescence emission spectra in the presence of increasing concentration of **DPA52** (A). The decrease of fluorescence intensity (at 610 nm) of the tetraloop TAR RNA mutant/EtBr complex with increasing concentration of **DPA52** results in a saturating binding plot (B). The plot between normalized fluorescence intensity (at 610 nm) of the tetraloop TAR RNA mutant-EtBr complex as a function of concentration of **DPA52** results in a saturating binding plot (C). The Scatchard plot analysis of **DPA52** with the tetraloop TAR RNA mutant (D). The plot between normalized EtBr displacement (at 610 nm) of the tetraloop TAR RNA mutant-EtBr complex as a function of concentration of **DPA52** (E). The plot for EtBr displacement (%) of the tetraloop TAR RNA mutant-EtBr complex versus the log of the **DPA52** r_{dr}, the data shown with a sigmoidal fit, was used to determine the IC_{50} value (F). Buffer conditions: 100 mM KCl, 10 mM SC, 0.5 mM EDTA, pH 6.8. Tetraloop TAR RNA mutant = 200 nM/strand. [EtBr] = 5 µM.

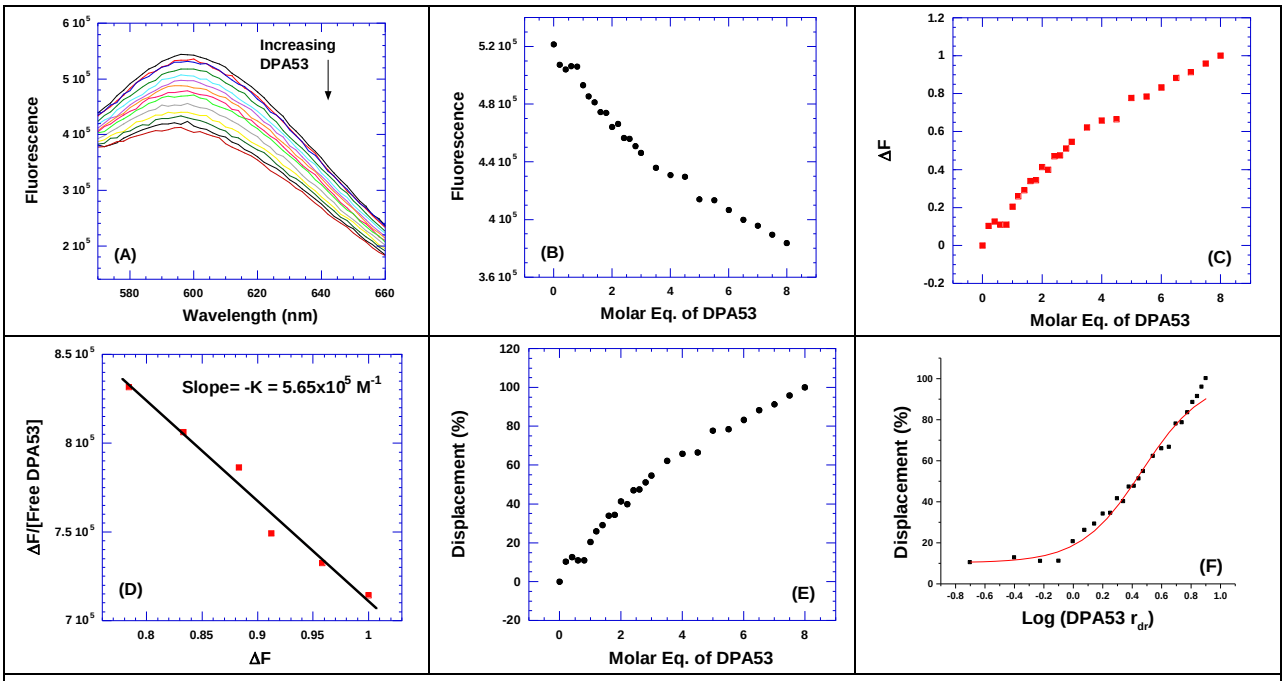

Figure S4.13. FID titration of **DPA53** with the **tetraloop TAR RNA mutant**. Raw fluorescence emission spectra in the presence of increasing concentration of **DPA53** (A). The decrease of fluorescence intensity (at 610 nm) of the tetraloop TAR RNA mutant/EtBr complex with increasing concentration of **DPA53** results in a saturating binding plot (B). The plot between normalized fluorescence intensity (at 610 nm) of the tetraloop TAR RNA mutant-EtBr complex as a function of concentration of **DPA53** results in a saturating binding plot (C). The Scatchard plot analysis of **DPA53** with the tetraloop TAR RNA mutant (D). The plot between normalized EtBr displacement (at 610 nm) of the tetraloop TAR RNA mutant-EtBr complex as a function of concentration of **DPA53** (E). The plot for EtBr displacement (%) of the tetraloop TAR RNA mutant-EtBr complex versus the log of the **DPA53** r_{dr}, the data shown with a sigmoidal fit, was used to determine the IC_{50} value (F). Buffer conditions: 100 mM KCl, 10 mM SC, 0.5 mM EDTA, pH 6.8. Tetraloop TAR RNA mutant = 200 nM/strand. [EtBr] = 5 µM.

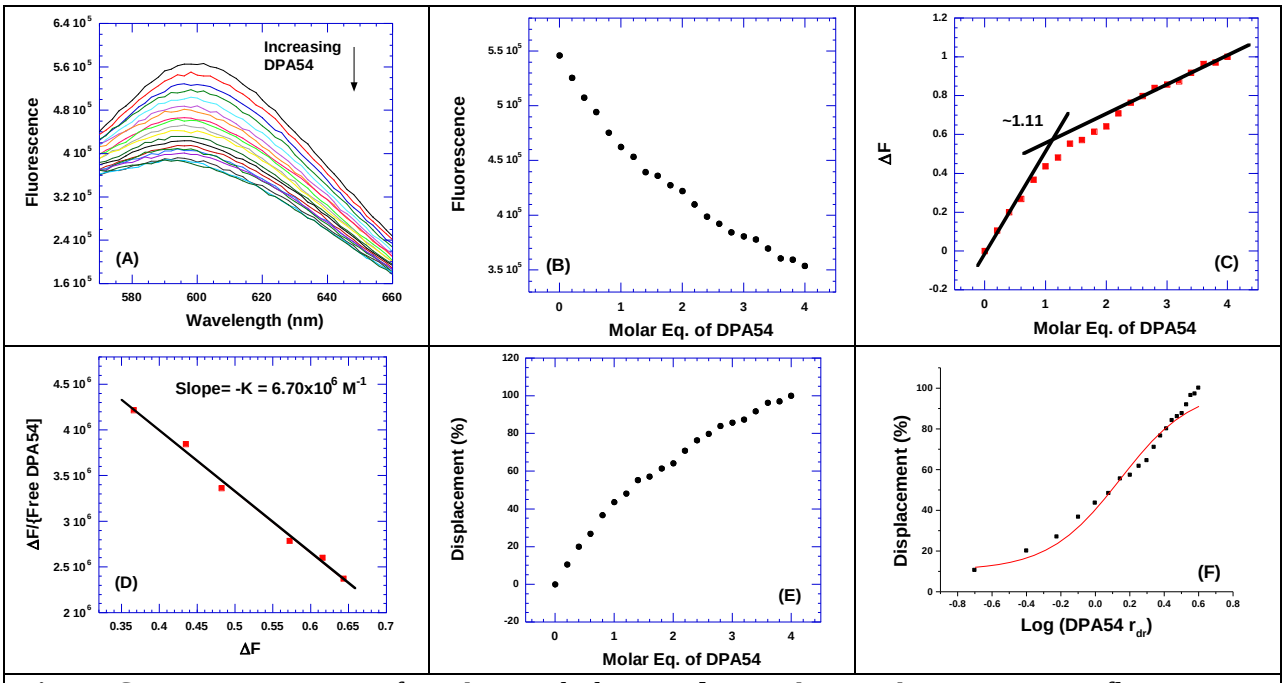

Figure S4.14. FID titration of **DPA54** with the **tetraloop TAR RNA mutant**. Raw fluorescence emission spectra in the presence of increasing concentration of **DPA54** (A). The decrease of fluorescence intensity (at 610 nm) of the tetraloop TAR RNA mutant/EtBr complex with increasing concentration of **DPA54** results in a saturating binding plot (B). The plot between normalized fluorescence intensity (at 610 nm) of the tetraloop TAR RNA mutant-EtBr complex as a function of concentration of **DPA54** results in a saturating binding plot (C). The Scatchard plot analysis of **DPA54** with the tetraloop TAR RNA mutant (D). The plot between normalized EtBr displacement (at 610 nm) of the tetraloop TAR RNA mutant-EtBr complex as a function of concentration of **DPA54** (E). The plot for EtBr displacement (%) of the tetraloop TAR RNA mutant-EtBr complex versus the log of the **DPA54** r_{dr}, the data shown with a sigmoidal fit, was used to determine the IC_{50} value (F). Buffer conditions: 100 mM KCl, 10 mM SC, 0.5 mM EDTA, pH 6.8. Tetraloop TAR RNA mutant = 200 nM/strand. [EtBr] = 5 µM.

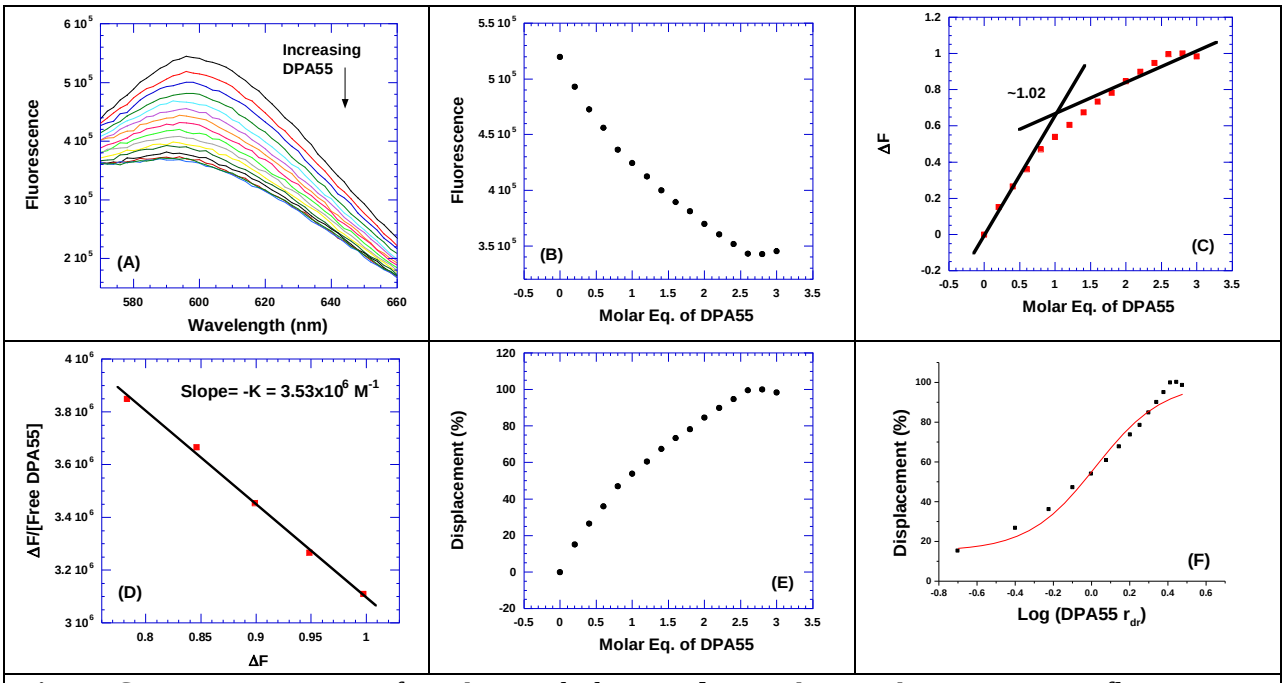

Figure S4.15. FID titration of **DPA55** with the **tetraloop TAR RNA mutant**. Raw fluorescence emission spectra in the presence of increasing concentration of **DPA55** (A). The decrease of fluorescence intensity (at 610 nm) of the tetraloop TAR RNA mutant/EtBr complex with increasing concentration of **DPA55** results in a saturating binding plot (B). The plot between normalized fluorescence intensity (at 610 nm) of the tetraloop TAR RNA mutant-EtBr complex as a function of concentration of **DPA55** results in a saturating binding plot (C). The Scatchard plot analysis of **DPA55** with the tetraloop TAR RNA mutant (D). The plot between normalized EtBr displacement (at 610 nm) of the tetraloop TAR RNA mutant-EtBr complex as a function of concentration of **DPA55** (E). The plot for EtBr displacement (%) of the tetraloop TAR RNA mutant-EtBr complex versus the log of the **DPA55** r_{dr}, the data shown with a sigmoidal fit, was used to determine the IC_{50} value (F). Buffer conditions: 100 mM KCl, 10 mM SC, 0.5 mM EDTA, pH 6.8. Tetraloop TAR RNA mutant = 200 nM/strand. [EtBr] = 5 µM.

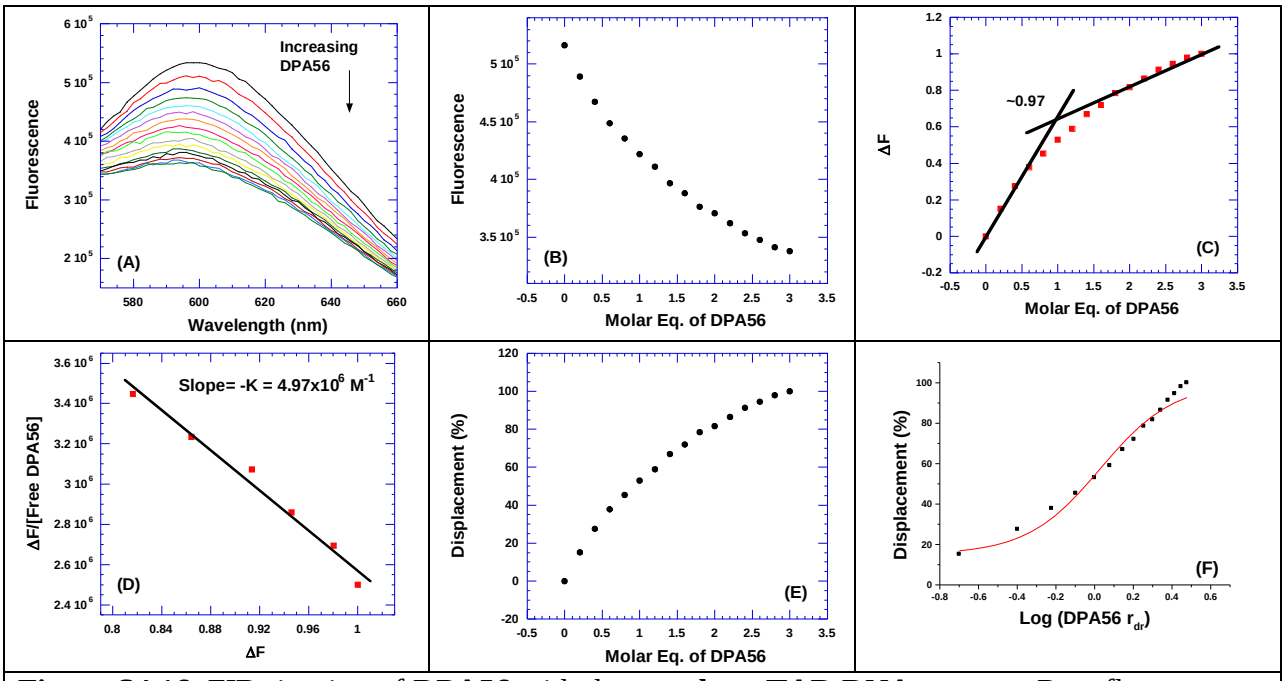

Figure S4.16. FID titration of **DPA56** with the **tetraloop TAR RNA mutant**. Raw fluorescence emission spectra in the presence of increasing concentration of **DPA56** (A). The decrease of fluorescence intensity (at 610 nm) of the tetraloop TAR RNA mutant/EtBr complex with increasing concentration of **DPA56** results in a saturating binding plot (B). The plot between normalized fluorescence intensity (at 610 nm) of the tetraloop TAR RNA mutant-EtBr complex as a function of concentration of **DPA56** results in a saturating binding plot (C). The Scatchard plot analysis of **DPA56** with the tetraloop TAR RNA mutant (D). The plot between normalized EtBr displacement (at 610 nm) of the tetraloop TAR RNA mutant-EtBr complex as a function of concentration of **DPA56** (E). The plot for EtBr displacement (%) of the tetraloop TAR RNA mutant-EtBr complex versus the log of the **DPA56** r_{dr}, the data shown with a sigmoidal fit, was used to determine the IC_{50} value (F). Buffer conditions: 100 mM KCl, 10 mM SC, 0.5 mM EDTA, pH 6.8. Tetraloop TAR RNA mutant = 200 nM/strand. [EtBr] = 5 µM.

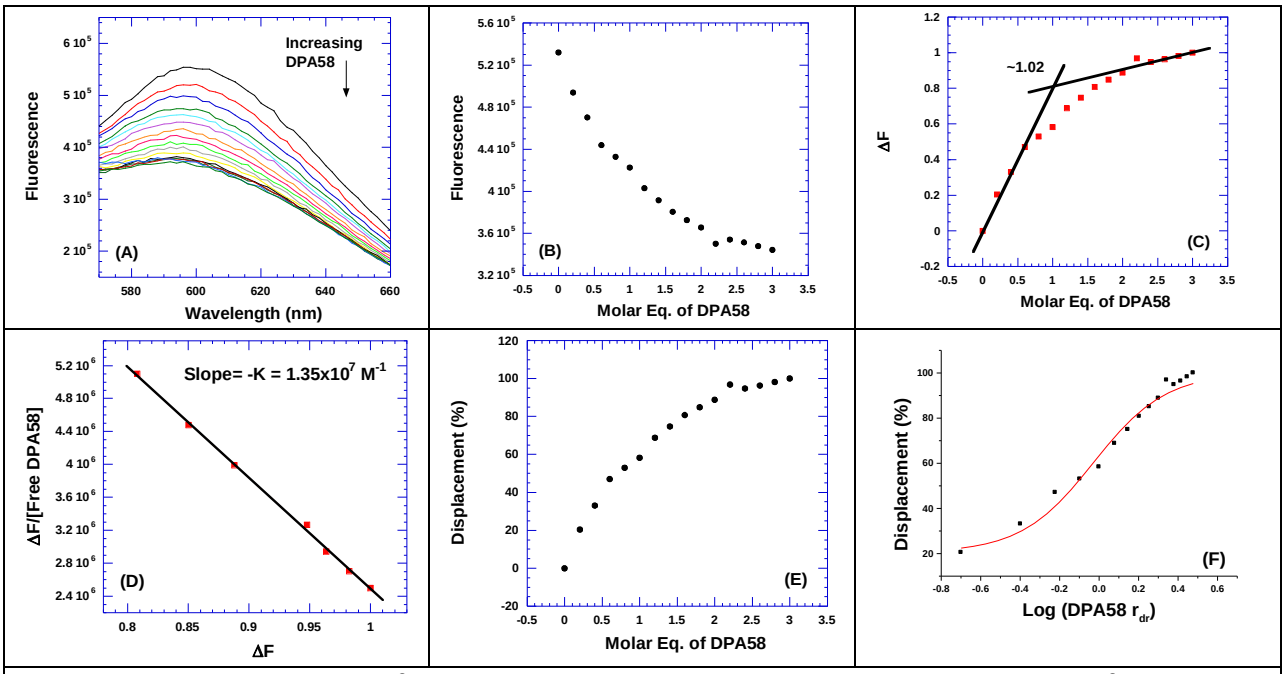

Figure S4.17. FID titration of **DPA58** with the **tetraloop TAR RNA mutant**. Raw fluorescence emission spectra in the presence of increasing concentration of **DPA58** (A). The decrease of fluorescence intensity (at 610 nm) of the tetraloop TAR RNA mutant/EtBr complex with increasing concentration of **DPA58** results in a saturating binding plot (B). The plot between normalized fluorescence intensity (at 610 nm) of the tetraloop TAR RNA mutant-EtBr complex as a function of concentration of **DPA58** results in a saturating binding plot (C). The Scatchard plot analysis of **DPA58** with the tetraloop TAR RNA mutant (D). The plot between normalized EtBr displacement (at 610 nm) of the tetraloop TAR RNA mutant-EtBr complex as a function of concentration of **DPA58** (E). The plot for EtBr displacement (%) of the tetraloop TAR RNA mutant-EtBr complex versus the log of the **DPA58** r_{dr}, the data shown with a sigmoidal fit, was used to determine the IC_{50} value (F). Buffer conditions: 100 mM KCl, 10 mM SC, 0.5 mM EDTA, pH 6.8. Tetraloop TAR RNA mutant = 200 nM/strand. [EtBr] = 5 µM.

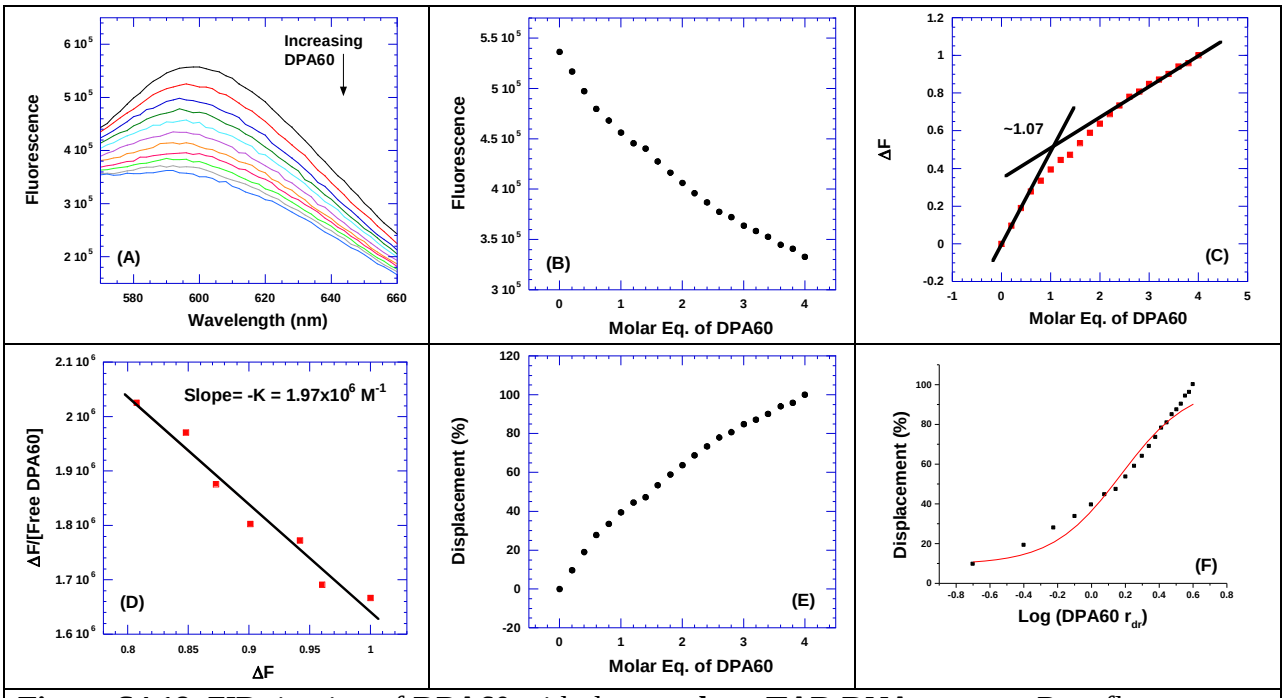

Figure S4.18. FID titration of **DPA60** with the **tetraloop TAR RNA mutant**. Raw fluorescence emission spectra in the presence of increasing concentration of **DPA60** (A). The decrease of fluorescence intensity (at 610 nm) of the tetraloop TAR RNA mutant/EtBr complex with increasing concentration of **DPA60** results in a saturating binding plot (B). The plot between normalized fluorescence intensity (at 610 nm) of the tetraloop TAR RNA mutant-EtBr complex as a function of concentration of **DPA60** results in a saturating binding plot (C). The Scatchard plot analysis of **DPA60** with the tetraloop TAR RNA mutant (D). The plot between normalized EtBr displacement (at 610 nm) of the tetraloop TAR RNA mutant-EtBr complex as a function of concentration of **DPA60** (E). The plot for EtBr displacement (%) of the tetraloop TAR RNA mutant-EtBr complex versus the log of the **DPA60** r_{dr}, the data shown with a sigmoidal fit, was used to determine the IC_{50} value (F). Buffer conditions: 100 mM KCl, 10 mM SC, 0.5 mM EDTA, pH 6.8. Tetraloop TAR RNA mutant = 200 nM/strand. [EtBr] = 5 µM.

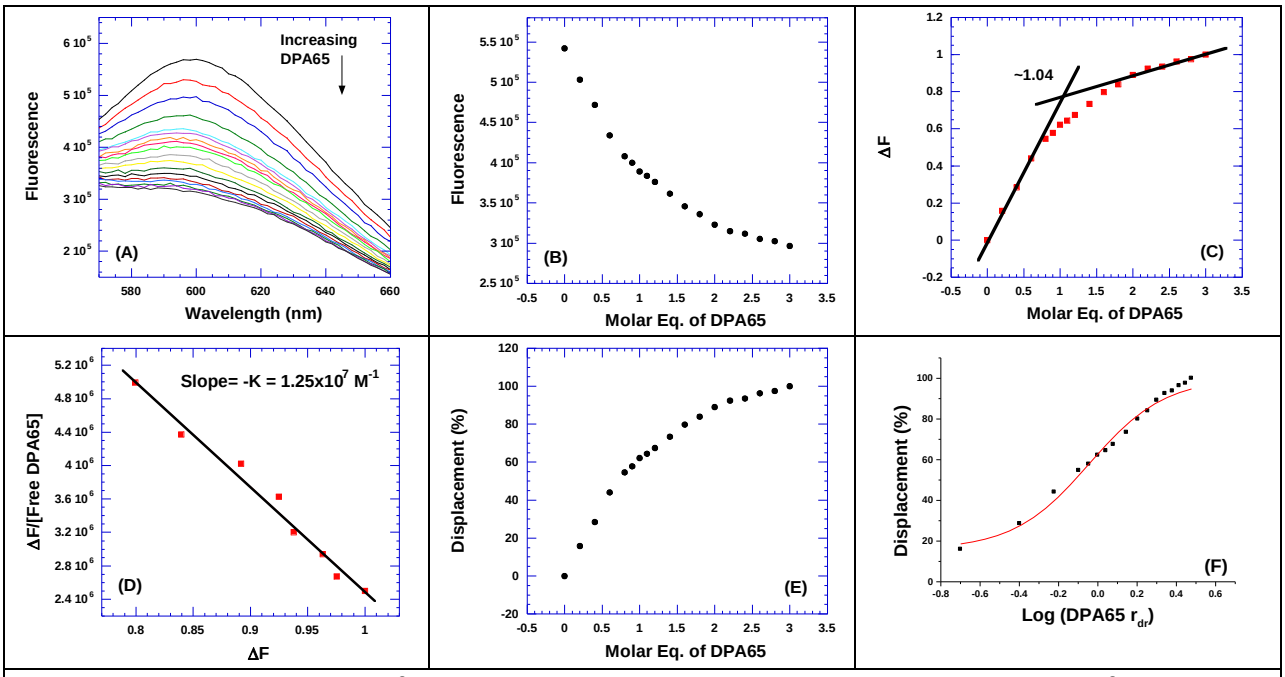

Figure S4.19. FID titration of **DPA65** with the **tetraloop TAR RNA mutant**. Raw fluorescence emission spectra in the presence of increasing concentration of **DPA65** (A). The decrease of fluorescence intensity (at 610 nm) of the tetraloop TAR RNA mutant/EtBr complex with increasing concentration of **DPA65** results in a saturating binding plot (B). The plot between normalized fluorescence intensity (at 610 nm) of the tetraloop TAR RNA mutant-EtBr complex as a function of concentration of **DPA65** results in a saturating binding plot (C). The Scatchard plot analysis of **DPA65** with the tetraloop TAR RNA mutant (D). The plot between normalized EtBr displacement (at 610 nm) of the tetraloop TAR RNA mutant-EtBr complex as a function of concentration of **DPA65** (E). The plot for EtBr displacement (%) of the tetraloop TAR RNA mutant-EtBr complex versus the log of the **DPA65** r_{dr}, the data shown with a sigmoidal fit, was used to determine the IC_{50} value (F). Buffer conditions: 100 mM KCl, 10 mM SC, 0.5 mM EDTA, pH 6.8. Tetraloop TAR RNA mutant = 200 nM/strand. [EtBr] = 5 µM.

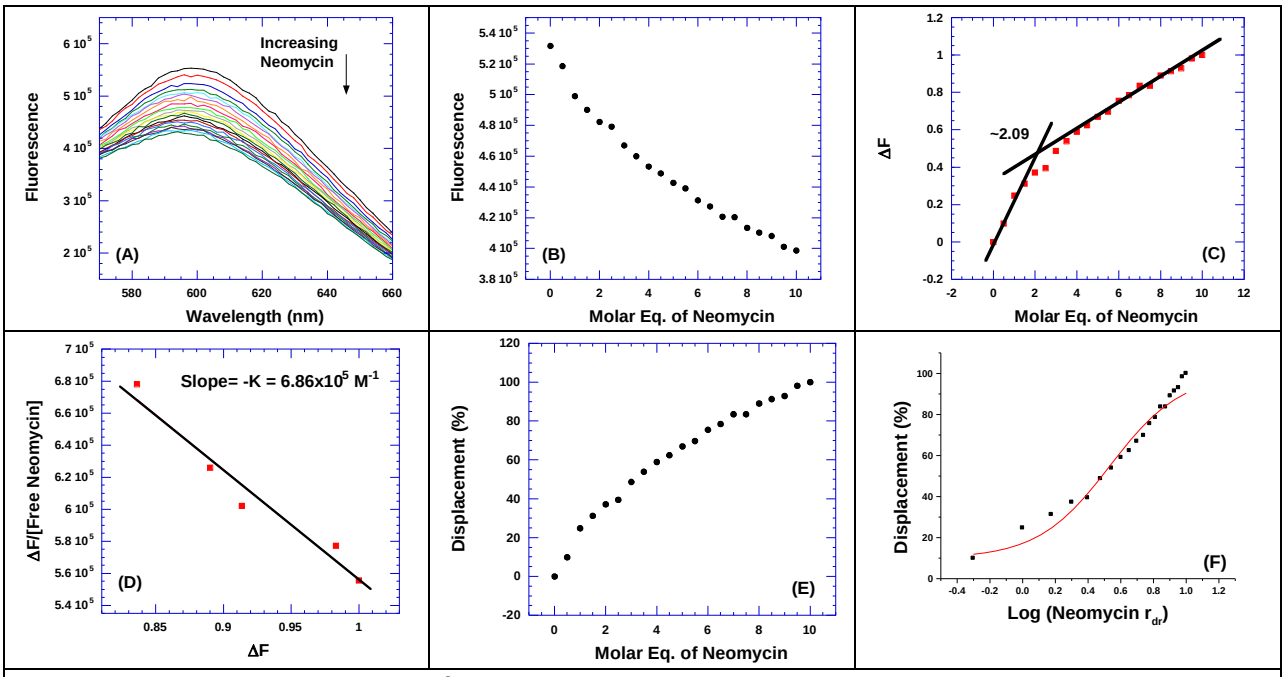

Figure S4.20. FID titration of **neomycin** with the **tetraloop TAR RNA mutant**. Raw fluorescence emission spectra in the presence of increasing concentration of **neomycin** (A). The decrease of fluorescence intensity (at 610 nm) of the tetraloop TAR RNA mutant/EtBr complex with increasing concentration of **neomycin** results in a saturating binding plot (B). The plot between normalized fluorescence intensity (at 610 nm) of the tetraloop TAR RNA mutant-EtBr complex as a function of concentration of **neomycin** results in a saturating binding plot (C). The Scatchard plot analysis of **neomycin** with the tetraloop TAR RNA mutant (D). The plot between normalized EtBr displacement (at 610 nm) of the tetraloop TAR RNA mutant-EtBr complex as a function of concentration of **neomycin** (E). The plot for EtBr displacement (%) of the tetraloop TAR RNA mutant-EtBr complex versus the log of the **neomycin** r_{dr}, the data shown with a sigmoidal fit, was used to determine the IC_{50} value (F). Buffer conditions: 100 mM KCl, 10 mM SC, 0.5 mM EDTA, pH 6.8. Tetraloop TAR RNA mutant = 200 nM/strand. [EtBr] = 5 µM.

Bulgeless Tetraloop TAR RNA Mutant Ethidium Bromide Displacement Binding Assay

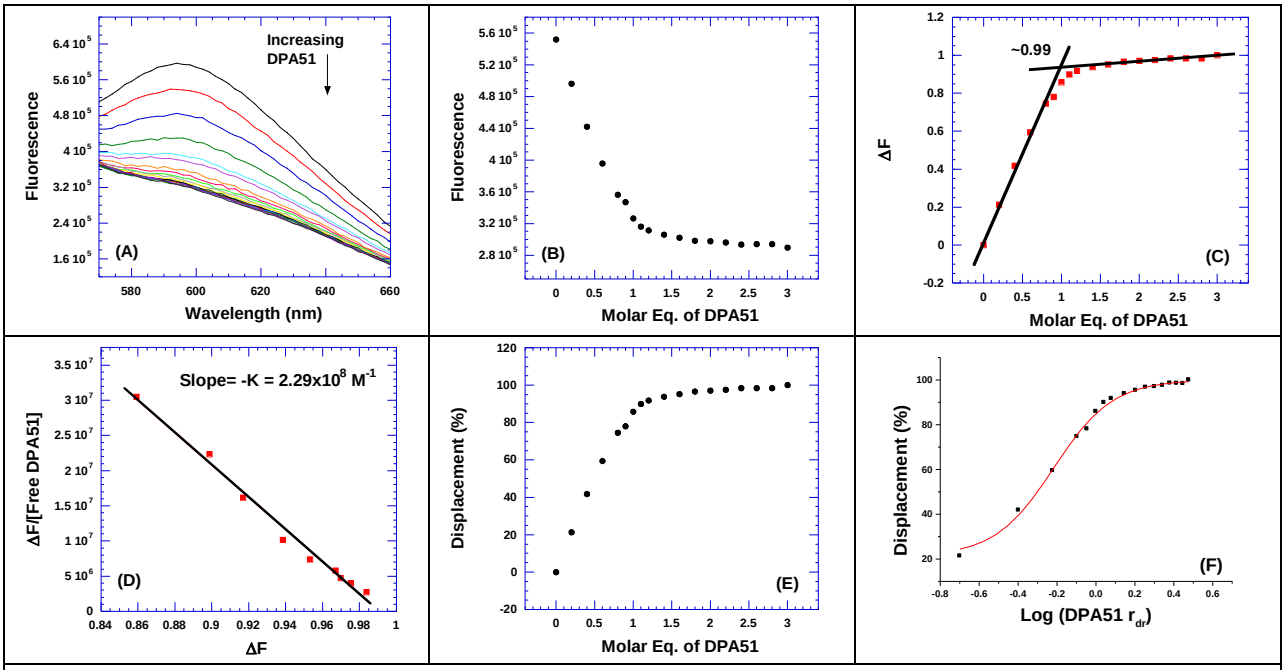

Figure S4.21. FID titration of **DPA51** with the **bulgeless tetraloop TAR RNA mutant**. Raw fluorescence emission spectra in the presence of increasing concentration of **DPA51** (A). The decrease of fluorescence intensity (at 610 nm) of the bulgeless tetraloop TAR RNA mutant/EtBr complex with increasing concentration of **DPA51** results in a saturating binding plot (B). The plot between normalized fluorescence intensity (at 610 nm) of the bulgeless tetraloop TAR RNA mutant-EtBr complex as a function of concentration of **DPA51** results in a saturating binding plot (C). The Scatchard plot analysis of **DPA51** with the bulgeless tetraloop TAR RNA mutant (D). The plot between normalized EtBr displacement (at 610 nm) of the bulgeless tetraloop TAR RNA mutant-EtBr complex as a function of concentration of **DPA51** (E). The plot for EtBr displacement (%) of the bulgeless tetraloop TAR RNA mutant-EtBr complex versus the log of the **DPA51** r_{dr}, the data shown with a sigmoidal fit, was used to determine the IC_{50} value (F). Buffer conditions: 100 mM KCl, 10 mM SC, 0.5 mM EDTA, pH 6.8. Bulgeless tetraloop TAR RNA mutant = 200 nM/strand. [EtBr] = 5 µM.

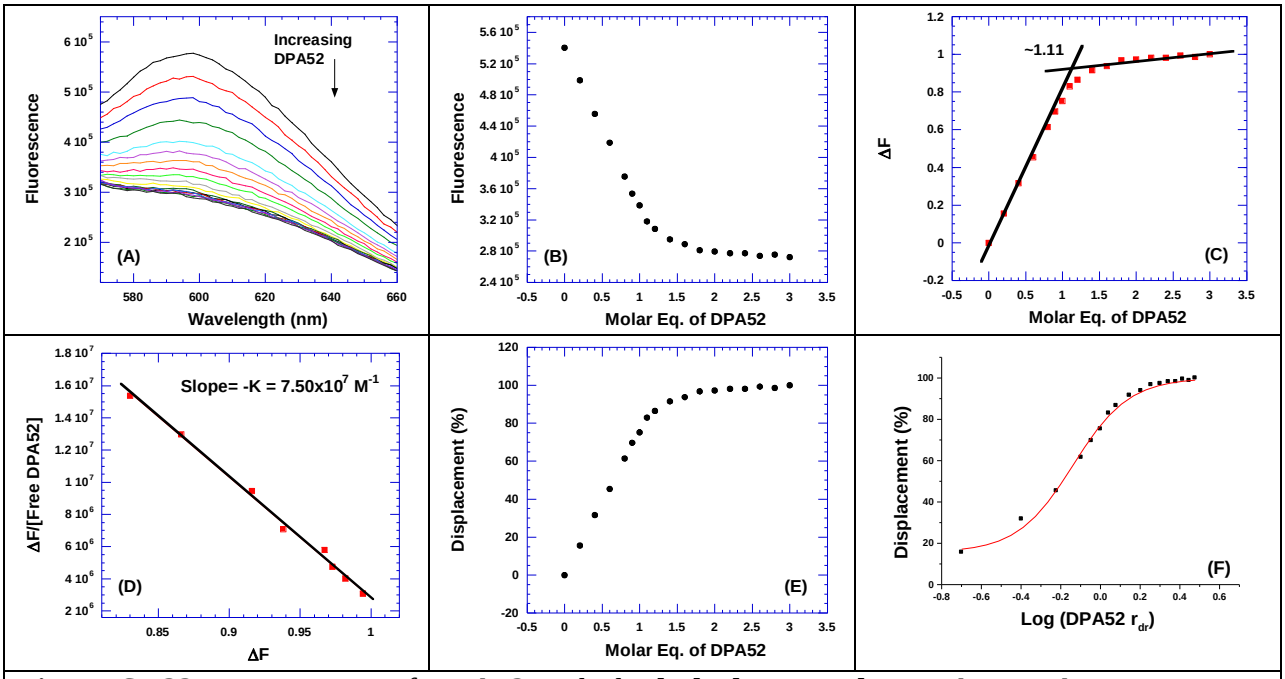

Figure S4.22. FID titration of **DPA52** with the **bulgeless tetraloop TAR RNA mutant**. Raw fluorescence emission spectra in the presence of increasing concentration of **DPA52** (A). The decrease of fluorescence intensity (at 610 nm) of the bulgeless tetraloop TAR RNA mutant/EtBr complex with increasing concentration of **DPA52** results in a saturating binding plot (B). The plot between normalized fluorescence intensity (at 610 nm) of the bulgeless tetraloop TAR RNA mutant-EtBr complex as a function of concentration of **DPA52** results in a saturating binding plot (C). The Scatchard plot analysis of **DPA52** with the bulgeless tetraloop TAR RNA mutant (D). The plot between normalized EtBr displacement (at 610 nm) of the bulgeless tetraloop TAR RNA mutant-EtBr complex as a function of concentration of **DPA52** (E). The plot for EtBr displacement (%) of the bulgeless tetraloop TAR RNA mutant-EtBr complex versus the log of the **DPA52** r_{dr}, the data shown with a sigmoidal fit, was used to determine the IC_{50} value (F). Buffer conditions: 100 mM KCl, 10 mM SC, 0.5 mM EDTA, pH 6.8. Bulgeless tetraloop TAR RNA mutant = 200 nM/strand. [EtBr] = 5 µM.

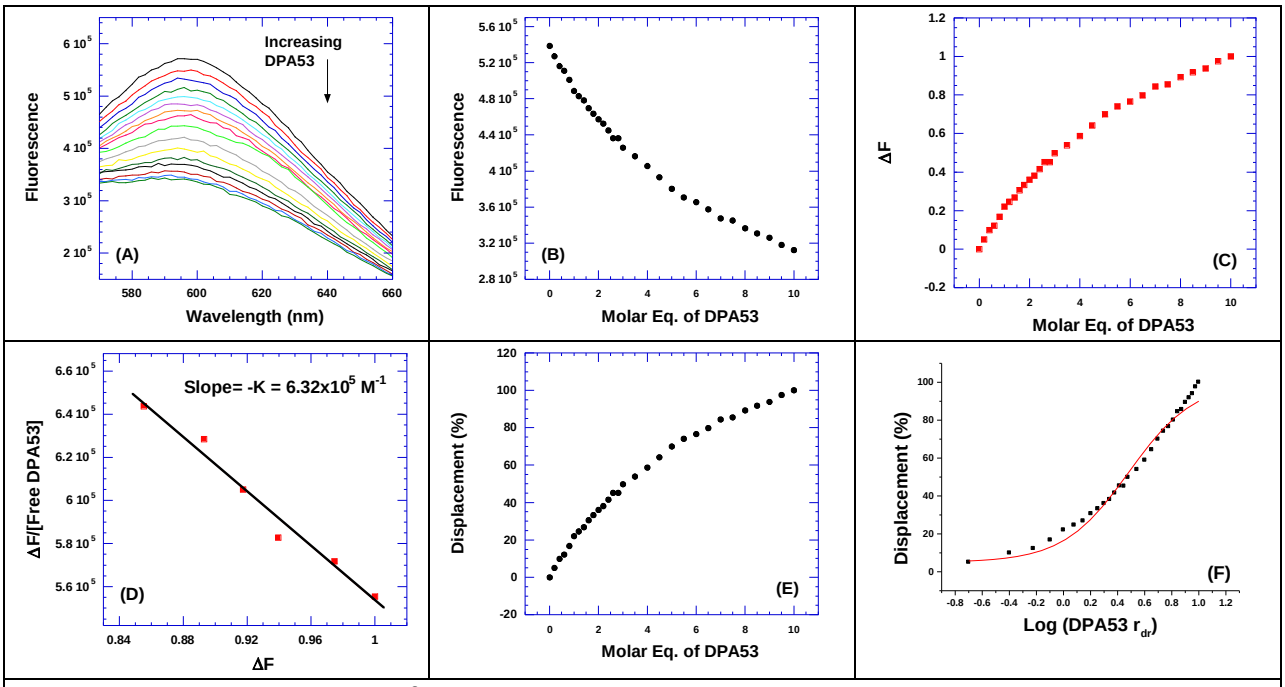

Figure S4.23. FID titration of **DPA53** with the **bulgeless tetraloop TAR RNA mutant**. Raw fluorescence emission spectra in the presence of increasing concentration of **DPA53** (A). The decrease of fluorescence intensity (at 610 nm) of the bulgeless tetraloop TAR RNA mutant/EtBr complex with increasing concentration of **DPA53** results in a saturating binding plot (B). The plot between normalized fluorescence intensity (at 610 nm) of the bulgeless tetraloop TAR RNA mutant-EtBr complex as a function of concentration of **DPA53** results in a saturating binding plot (C). The Scatchard plot analysis of **DPA53** with the bulgeless tetraloop TAR RNA mutant (D). The plot between normalized EtBr displacement (at 610 nm) of the bulgeless tetraloop TAR RNA mutant-EtBr complex as a function of concentration of **DPA53** (E). The plot for EtBr displacement (%) of the bulgeless tetraloop TAR RNA mutant-EtBr complex versus the log of the **DPA53** r_{dr}, the data shown with a sigmoidal fit, was used to determine the IC_{50} value (F). Buffer conditions: 100 mM KCl, 10 mM SC, 0.5 mM EDTA, pH 6.8. Bulgeless tetraloop TAR RNA mutant = 200 nM/strand. [EtBr] = 5 µM.

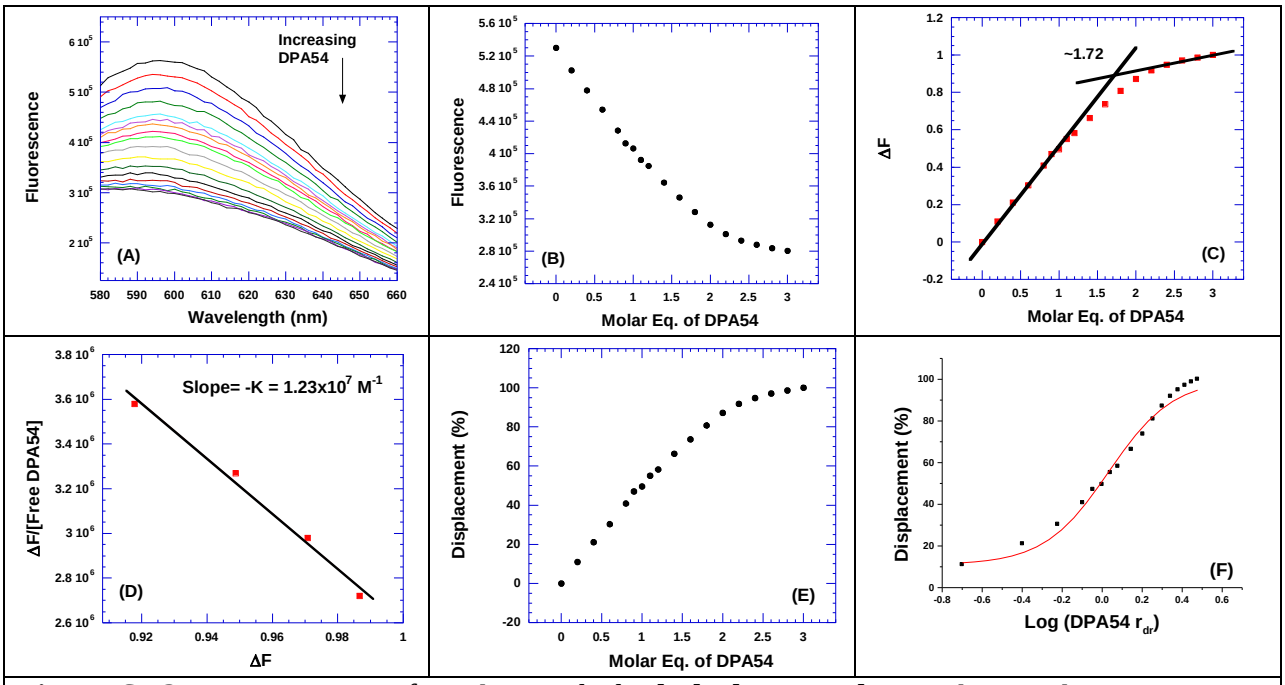

Figure S4.24. FID titration of **DPA54** with the **bulgeless tetraloop TAR RNA mutant**. Raw fluorescence emission spectra in the presence of increasing concentration of **DPA54** (A). The decrease of fluorescence intensity (at 610 nm) of the bulgeless tetraloop TAR RNA mutant/EtBr complex with increasing concentration of **DPA54** results in a saturating binding plot (B). The plot between normalized fluorescence intensity (at 610 nm) of the bulgeless tetraloop TAR RNA mutant-EtBr complex as a function of concentration of **DPA54** results in a saturating binding plot (C). The Scatchard plot analysis of **DPA54** with the bulgeless tetraloop TAR RNA mutant (D). The plot between normalized EtBr displacement (at 610 nm) of the bulgeless tetraloop TAR RNA mutant-EtBr complex as a function of concentration of **DPA54** (E). The plot for EtBr displacement (%) of the bulgeless tetraloop TAR RNA mutant-EtBr complex versus the log of the **DPA54** r_{dr}, the data shown with a sigmoidal fit, was used to determine the IC_{50} value (F). Buffer conditions: 100 mM KCl, 10 mM SC, 0.5 mM EDTA, pH 6.8. Bulgeless tetraloop TAR RNA mutant = 200 nM/strand. [EtBr] = 5 µM.

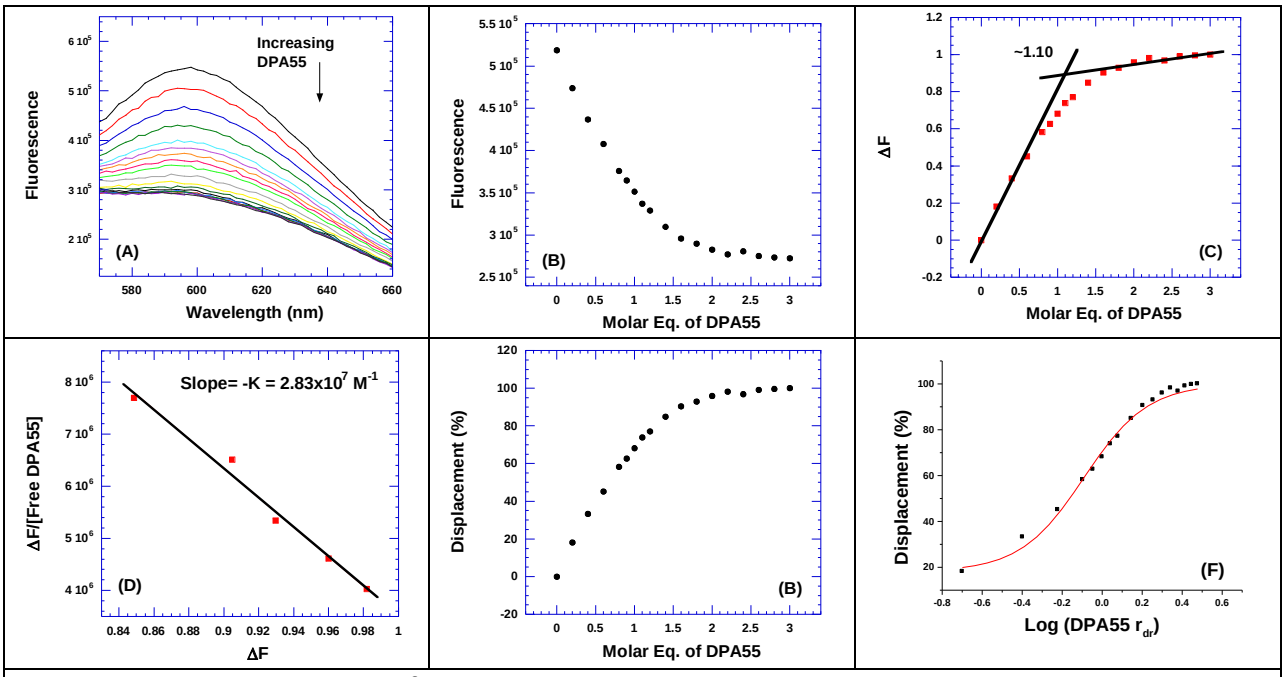

Figure S4.25. FID titration of **DPA55** with the **bulgeless tetraloop TAR RNA mutant**. Raw fluorescence emission spectra in the presence of increasing concentration of **DPA55** (A). The decrease of fluorescence intensity (at 610 nm) of the bulgeless tetraloop TAR RNA mutant/EtBr complex with increasing concentration of **DPA55** results in a saturating binding plot (B). The plot between normalized fluorescence intensity (at 610 nm) of the bulgeless tetraloop TAR RNA mutant-EtBr complex as a function of concentration of **DPA55** results in a saturating binding plot (C). The Scatchard plot analysis of **DPA55** with the bulgeless tetraloop TAR RNA mutant (D). The plot between normalized EtBr displacement (at 610 nm) of the bulgeless tetraloop TAR RNA mutant-EtBr complex as a function of concentration of **DPA55** (E). The plot for EtBr displacement (%) of the bulgeless tetraloop TAR RNA mutant-EtBr complex versus the log of the **DPA55** r_{dr}, the data shown with a sigmoidal fit, was used to determine the IC_{50} value (F). Buffer conditions: 100 mM KCl, 10 mM SC, 0.5 mM EDTA, pH 6.8. Bulgeless tetraloop TAR RNA mutant = 200 nM/strand. [EtBr] = 5 µM.

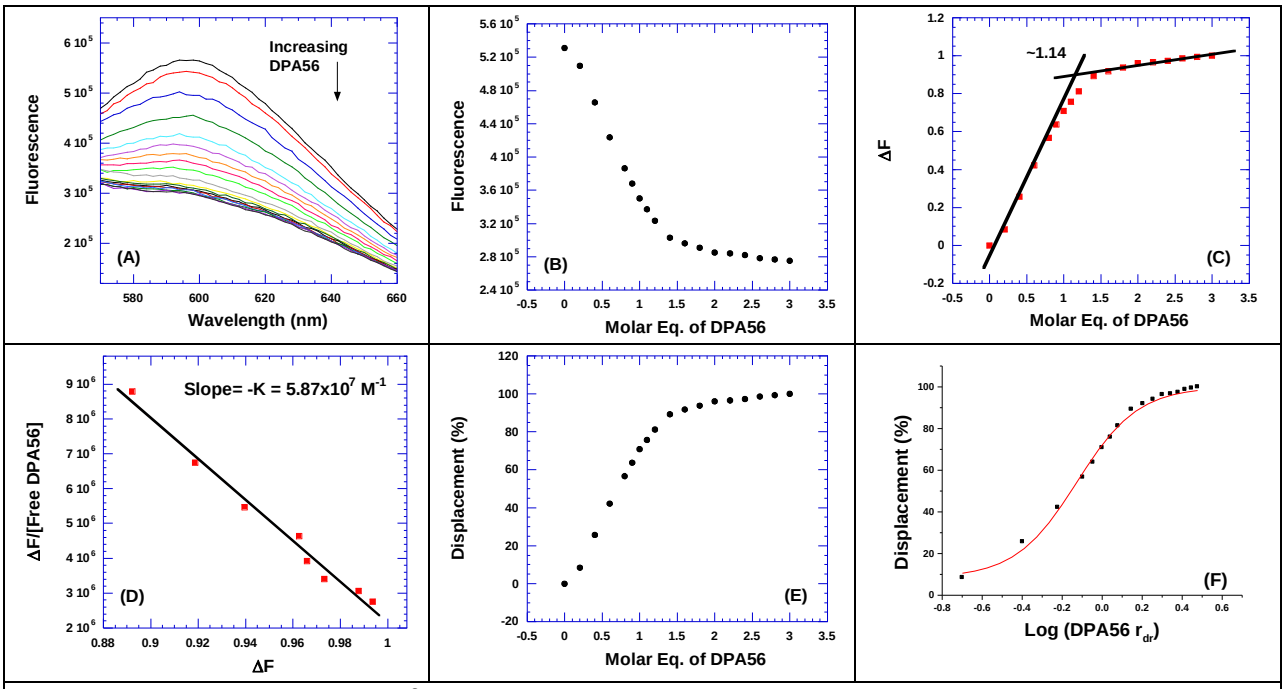

Figure S4.26. FID titration of **DPA56** with the **bulgeless tetraloop TAR RNA mutant**. Raw fluorescence emission spectra in the presence of increasing concentration of **DPA56** (A). The decrease of fluorescence intensity (at 610 nm) of the bulgeless tetraloop TAR RNA mutant/EtBr complex with increasing concentration of **DPA56** results in a saturating binding plot (B). The plot between normalized fluorescence intensity (at 610 nm) of the bulgeless tetraloop TAR RNA mutant-EtBr complex as a function of concentration of **DPA56** results in a saturating binding plot (C). The Scatchard plot analysis of **DPA56** with the bulgeless tetraloop TAR RNA mutant (D). The plot between normalized EtBr displacement (at 610 nm) of the bulgeless tetraloop TAR RNA mutant-EtBr complex as a function of concentration of **DPA56** (E). The plot for EtBr displacement (%) of the bulgeless tetraloop TAR RNA mutant-EtBr complex versus the log of the **DPA56** r_{dr}, the data shown with a sigmoidal fit, was used to determine the IC_{50} value (F). Buffer conditions: 100 mM KCl, 10 mM SC, 0.5 mM EDTA, pH 6.8. Bulgeless tetraloop TAR RNA mutant = 200 nM/strand. [EtBr] = 5 µM.

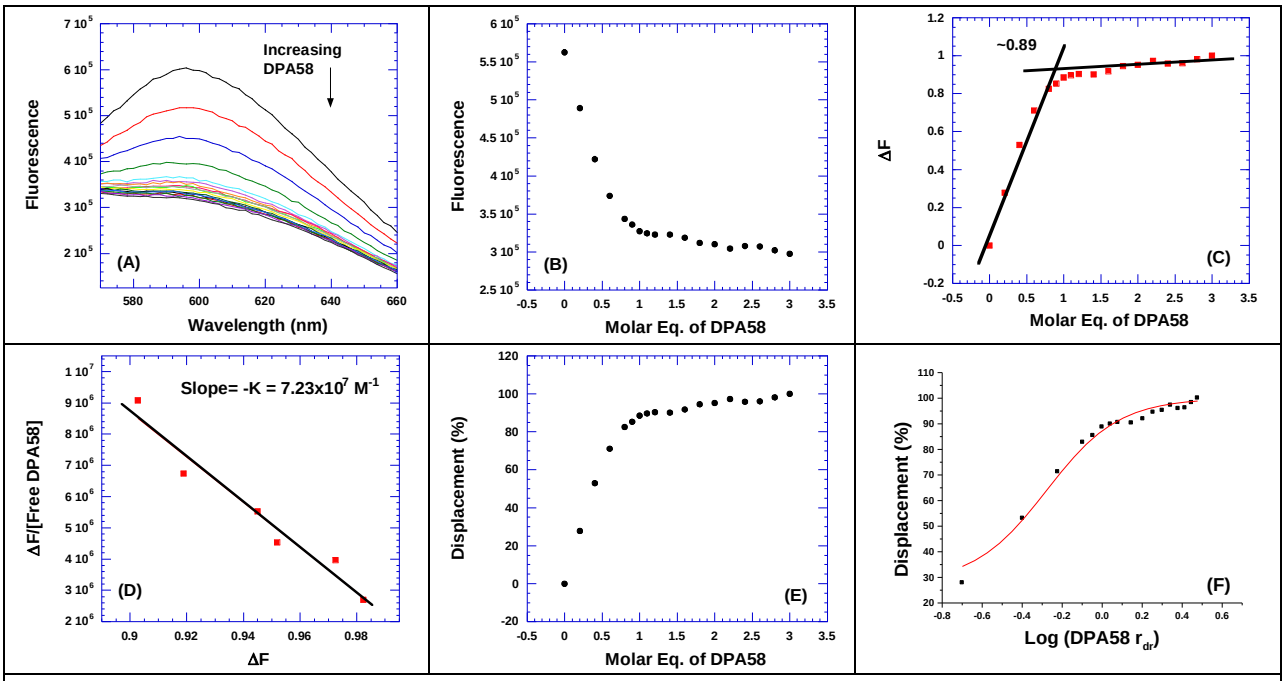

Figure S4.27. FID titration of **DPA58** with the **bulgeless tetraloop TAR RNA mutant**. Raw fluorescence emission spectra in the presence of increasing concentration of **DPA58** (A). The decrease of fluorescence intensity (at 610 nm) of the bulgeless tetraloop TAR RNA mutant/EtBr complex with increasing concentration of **DPA58** results in a saturating binding plot (B). The plot between normalized fluorescence intensity (at 610 nm) of the bulgeless tetraloop TAR RNA mutant-EtBr complex as a function of concentration of **DPA58** results in a saturating binding plot (C). The Scatchard plot analysis of **DPA58** with the bulgeless tetraloop TAR RNA mutant (D). The plot between normalized EtBr displacement (at 610 nm) of the bulgeless tetraloop TAR RNA mutant-EtBr complex as a function of concentration of **DPA58** (E). The plot for EtBr displacement (%) of the bulgeless tetraloop TAR RNA mutant-EtBr complex versus the log of the **DPA58** r_{dr}, the data shown with a sigmoidal fit, was used to determine the IC_{50} value (F). Buffer conditions: 100 mM KCl, 10 mM SC, 0.5 mM EDTA, pH 6.8. Bulgeless tetraloop TAR RNA mutant = 200 nM/strand. [EtBr] = 5 µM.

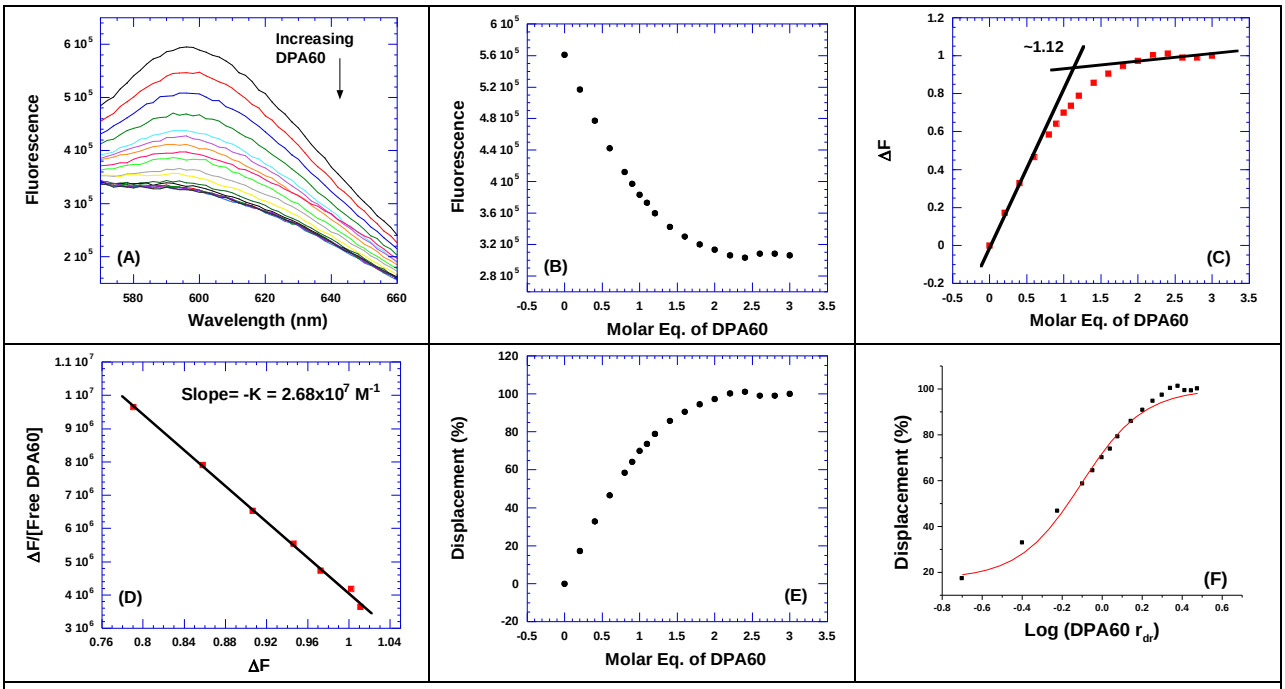

Figure S4.28. FID titration of **DPA60** with the **bulgeless tetraloop TAR RNA mutant**. Raw fluorescence emission spectra in the presence of increasing concentration of **DPA60** (A). The decrease of fluorescence intensity (at 610 nm) of the bulgeless tetraloop TAR RNA mutant/EtBr complex with increasing concentration of **DPA60** results in a saturating binding plot (B). The plot between normalized fluorescence intensity (at 610 nm) of the bulgeless tetraloop TAR RNA mutant-EtBr complex as a function of concentration of **DPA60** results in a saturating binding plot (C). The Scatchard plot analysis of **DPA60** with the bulgeless tetraloop TAR RNA mutant (D). The plot between normalized EtBr displacement (at 610 nm) of the bulgeless tetraloop TAR RNA mutant-EtBr complex as a function of concentration of **DPA60** (E). The plot for EtBr displacement (%) of the bulgeless tetraloop TAR RNA mutant-EtBr complex versus the log of the **DPA60** r_{dr}, the data shown with a sigmoidal fit, was used to determine the IC_{50} value (F). Buffer conditions: 100 mM KCl, 10 mM SC, 0.5 mM EDTA, pH 6.8. Bulgeless tetraloop TAR RNA mutant = 200 nM/strand. [EtBr] = 5 µM.

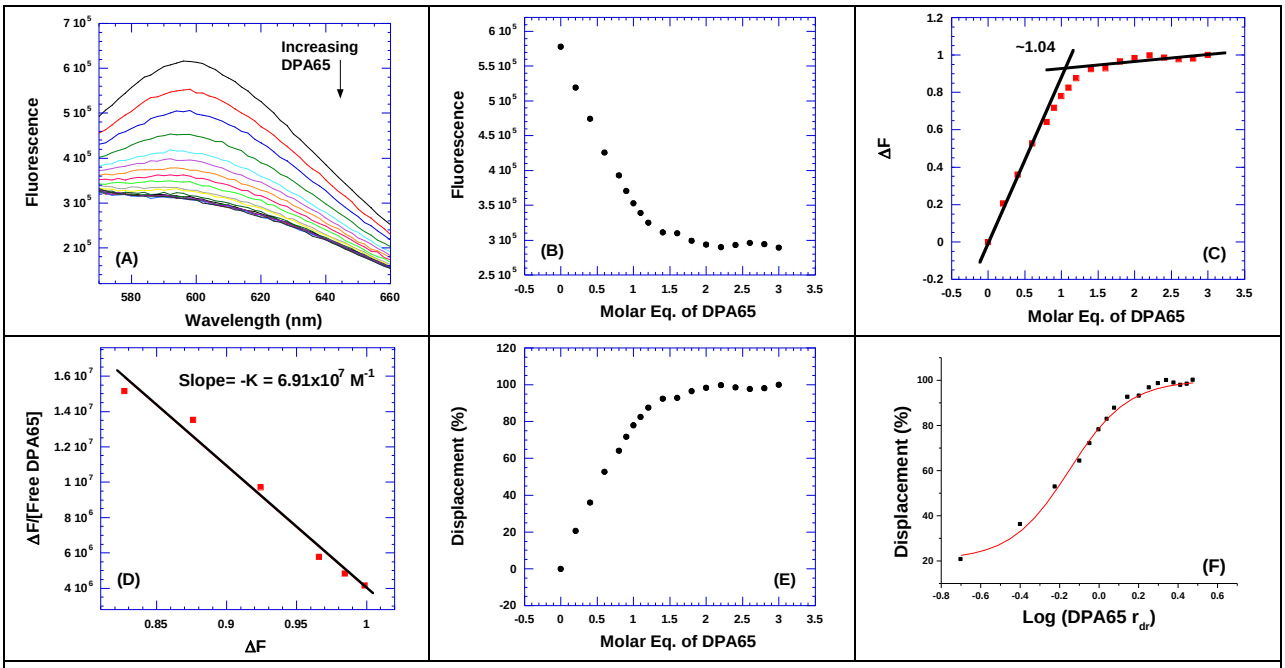

Figure S4.29. FID titration of **DPA65** with the **bulgeless tetraloop TAR RNA mutant**. Raw fluorescence emission spectra in the presence of increasing concentration of **DPA65** (A). The decrease of fluorescence intensity (at 610 nm) of the bulgeless tetraloop TAR RNA mutant/EtBr complex with increasing concentration of **DPA65** results in a saturating binding plot (B). The plot between normalized fluorescence intensity (at 610 nm) of the bulgeless tetraloop TAR RNA mutant-EtBr complex as a function of concentration of **DPA65** results in a saturating binding plot (C). The Scatchard plot analysis of **DPA65** with the bulgeless tetraloop TAR RNA mutant (D). The plot between normalized EtBr displacement (at 610 nm) of the bulgeless tetraloop TAR RNA mutant-EtBr complex as a function of concentration of **DPA65** (E). The plot for EtBr displacement (%) of the bulgeless tetraloop TAR RNA mutant-EtBr complex versus the log of the **DPA65** r_{dr}, the data shown with a sigmoidal fit, was used to determine the IC_{50} value (F). Buffer conditions: 100 mM KCl, 10 mM SC, 0.5 mM EDTA, pH 6.8. Bulgeless tetraloop TAR RNA mutant = 200 nM/strand. [EtBr] = 5 µM.

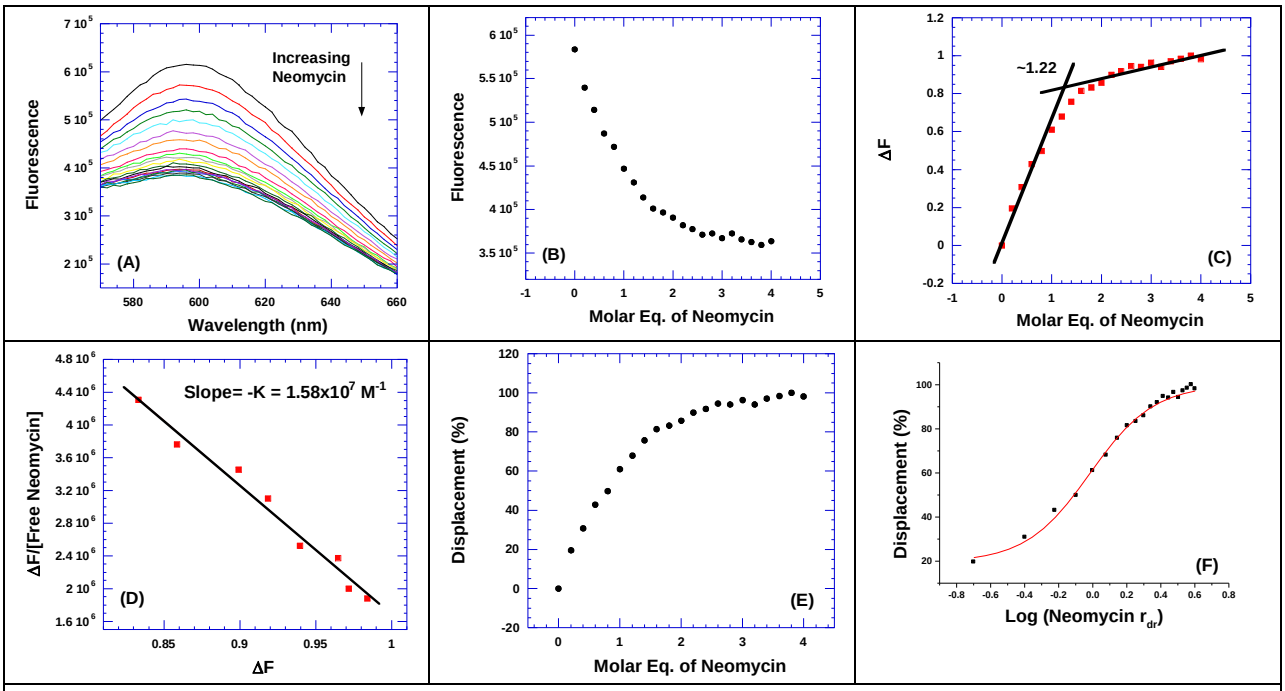

Figure S4.30. FID titration of **neomycin** with the **bulgeless tetraloop TAR RNA mutant**. Raw fluorescence emission spectra in the presence of increasing concentration of **neomycin** (A). The decrease of fluorescence intensity (at 610 nm) of the bulgeless tetraloop TAR RNA mutant/EtBr complex with increasing concentration of **neomycin** results in a saturating binding plot (B). The plot between normalized fluorescence intensity (at 610 nm) of the bulgeless tetraloop TAR RNA mutant-EtBr complex as a function of concentration of **neomycin** results in a saturating binding plot (C). The Scatchard plot analysis of **neomycin** with the bulgeless tetraloop TAR RNA mutant (D). The plot between normalized EtBr displacement (at 610 nm) of the bulgeless tetraloop TAR RNA mutant-EtBr complex as a function of concentration of **neomycin** (E). The plot for EtBr displacement (%) of the bulgeless tetraloop TAR RNA mutant-EtBr complex versus the log of the **neomycin** r_{dr}, the data shown with a sigmoidal fit, was used to determine the IC_{50} value (F). Buffer conditions: 100 mM KCl, 10 mM SC, 0.5 mM EDTA, pH 6.8. Bulgeless tetraloop TAR RNA mutant = 200 nM/strand. [EtBr] = 5 μM.

U3 Bulge TAR RNA Mutant Ethidium Bromide Displacement Binding Assay

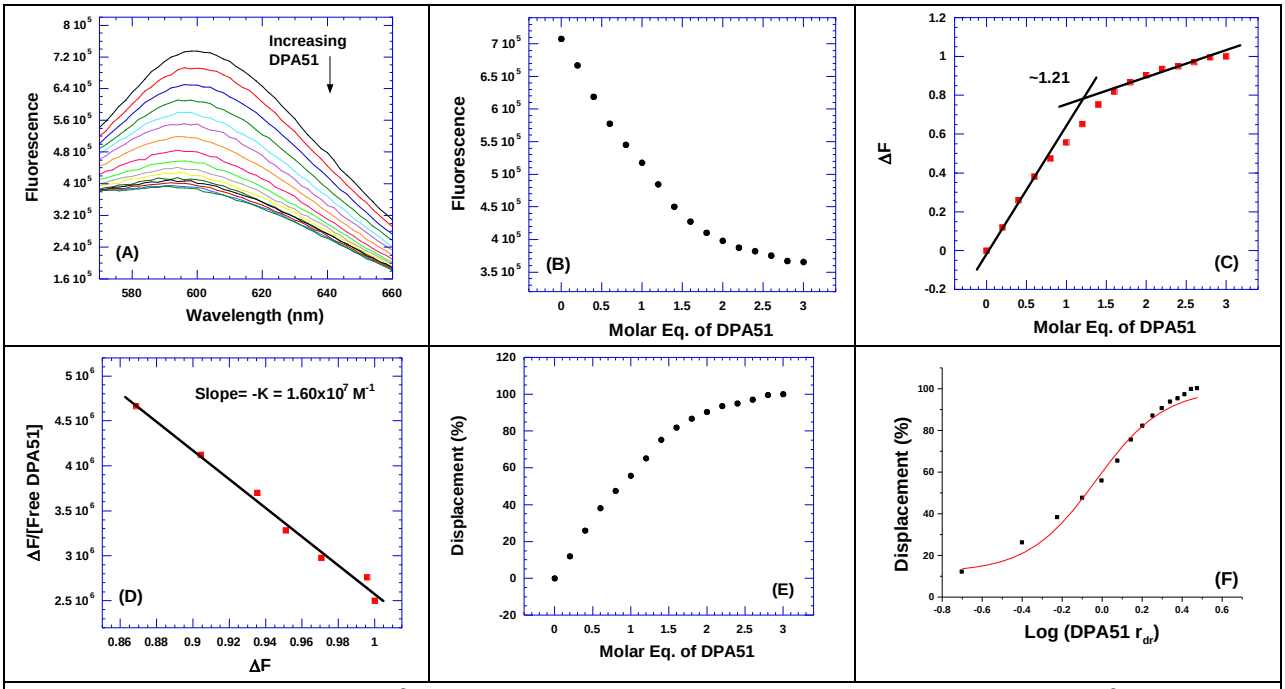

Figure S4.31. FID titration of **DPA51** with the **U3 bulge TAR RNA mutant**. Raw fluorescence emission spectra in the presence of increasing concentration of **DPA51** (A). The decrease of fluorescence intensity (at 610 nm) of the U3 bulge TAR RNA mutant/EtBr complex with increasing concentration of **DPA51** results in a saturating binding plot (B). The plot between normalized fluorescence intensity (at 610 nm) of the U3 bulge TAR RNA mutant-EtBr complex as a function of concentration of **DPA51** results in a saturating binding plot (C). The Scatchard plot analysis of **DPA51** with the U3 bulge TAR RNA mutant (D). The plot between normalized EtBr displacement (at 610 nm) of the U3 bulge TAR RNA mutant-EtBr complex as a function of concentration of **DPA51** (E). The plot for EtBr displacement (%) of the U3 bulge TAR RNA mutant-EtBr complex versus the log of the **DPA51** r_{dr}, the data shown with a sigmoidal fit, was used to determine the IC_{50} value (F). Buffer conditions: 100 mM KCl, 10 mM SC, 0.5 mM EDTA, pH 6.8. U3 bulge TAR RNA mutant = 200 nM/strand. [EtBr] = 5 µM.

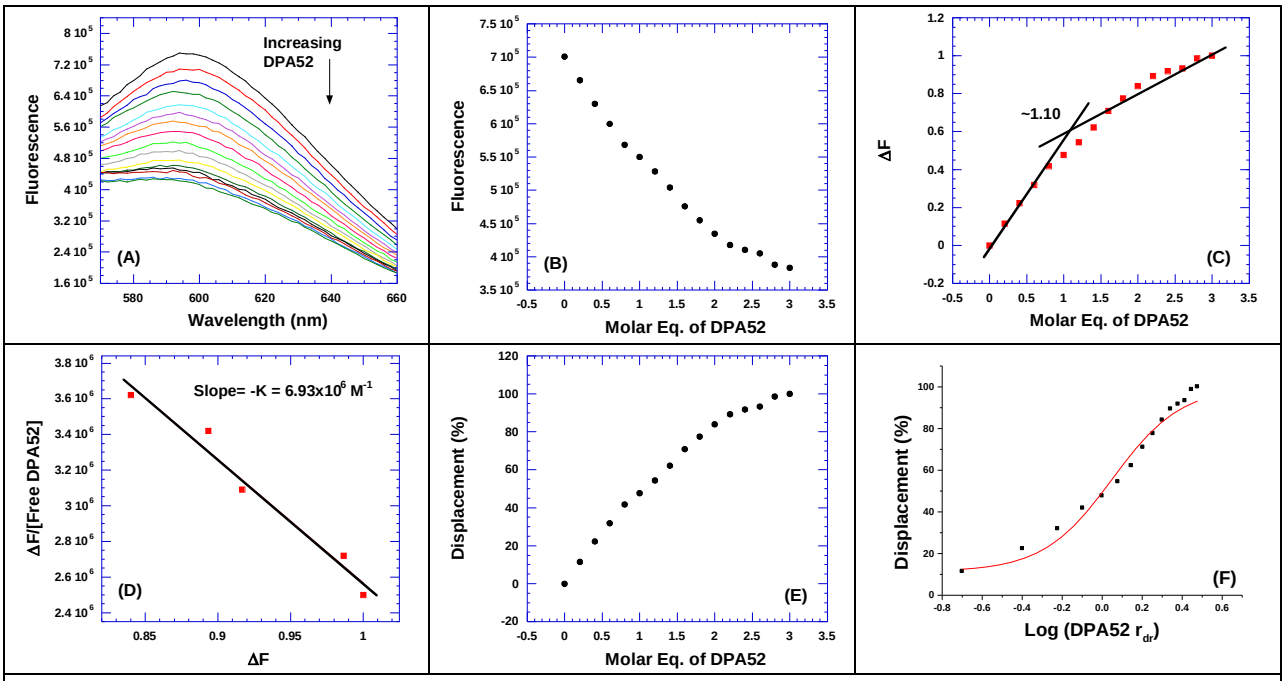

Figure S4.32. FID titration of **DPA52** with the **U3 bulge TAR RNA mutant**. Raw fluorescence emission spectra in the presence of increasing concentration of **DPA52** (A). The decrease of fluorescence intensity (at 610 nm) of the U3 bulge TAR RNA mutant/EtBr complex with increasing concentration of **DPA52** results in a saturating binding plot (B). The plot between normalized fluorescence intensity (at 610 nm) of the U3 bulge TAR RNA mutant-EtBr complex as a function of concentration of **DPA52** results in a saturating binding plot (C). The Scatchard plot analysis of **DPA52** with the U3 bulge TAR RNA mutant (D). The plot between normalized EtBr displacement (at 610 nm) of the U3 bulge TAR RNA mutant-EtBr complex as a function of concentration of **DPA52** (E). The plot for EtBr displacement (%) of the U3 bulge TAR RNA mutant-EtBr complex versus the log of the **DPA52** r_{dr}, the data shown with a sigmoidal fit, was used to determine the IC_{50} value (F). Buffer conditions: 100 mM KCl, 10 mM SC, 0.5 mM EDTA, pH 6.8. U3 bulge TAR RNA mutant = 200 nM/strand. [EtBr] = 5 µM.

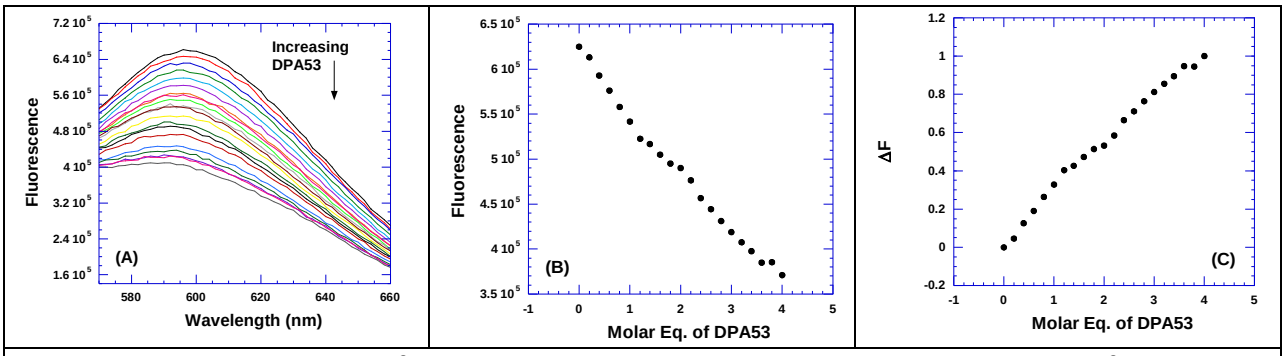

Figure S4.33. FID titration of **DPA53** with the **U3 bulge TAR RNA mutant**. Raw fluorescence emission spectra in the presence of increasing concentration of **DPA53** (A). The decrease of fluorescence intensity (at 610 nm) of the U3 bulge TAR RNA mutant/EtBr complex with increasing concentration of **DPA53** (B). The plot between normalized fluorescence intensity (at 610 nm) of the U3 bulge TAR RNA mutant-EtBr complex as a function of concentration of **DPA53** (C). Buffer conditions: 100 mM KCl, 10 mM SC, 0.5 mM EDTA, pH 6.8. U3 bulge TAR RNA mutant = 200 nM/strand. [EtBr] = 5 µM.

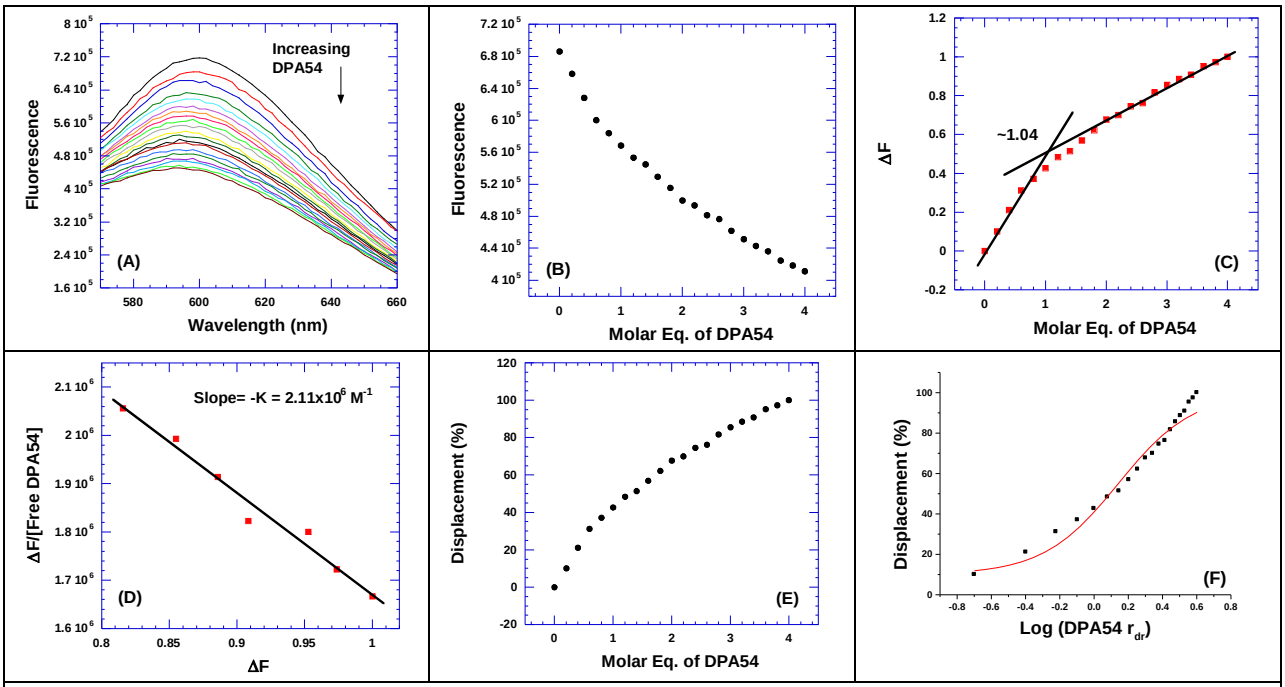

Figure S4.34. FID titration of **DPA54** with the **U3 bulge TAR RNA mutant**. Raw fluorescence emission spectra in the presence of increasing concentration of **DPA54** (A). The decrease of fluorescence intensity (at 610 nm) of the U3 bulge TAR RNA mutant/EtBr complex with increasing concentration of **DPA54** results in a saturating binding plot (B). The plot between normalized fluorescence intensity (at 610 nm) of the U3 bulge TAR RNA mutant-EtBr complex as a function of concentration of **DPA54** results in a saturating binding plot (C). The Scatchard plot analysis of **DPA54** with the U3 bulge TAR RNA mutant (D). The plot between normalized EtBr displacement (at 610 nm) of the U3 bulge TAR RNA mutant-EtBr complex as a function of concentration of **DPA54** (E). The plot for EtBr displacement (%) of the U3 bulge TAR RNA mutant-EtBr complex versus the log of the **DPA54** r_{dr}, the data shown with a sigmoidal fit, was used to determine the IC_{50} value (F). Buffer conditions: 100 mM KCl, 10 mM SC, 0.5 mM EDTA, pH 6.8. U3 bulge TAR RNA mutant = 200 nM/strand. [EtBr] = 5 µM.

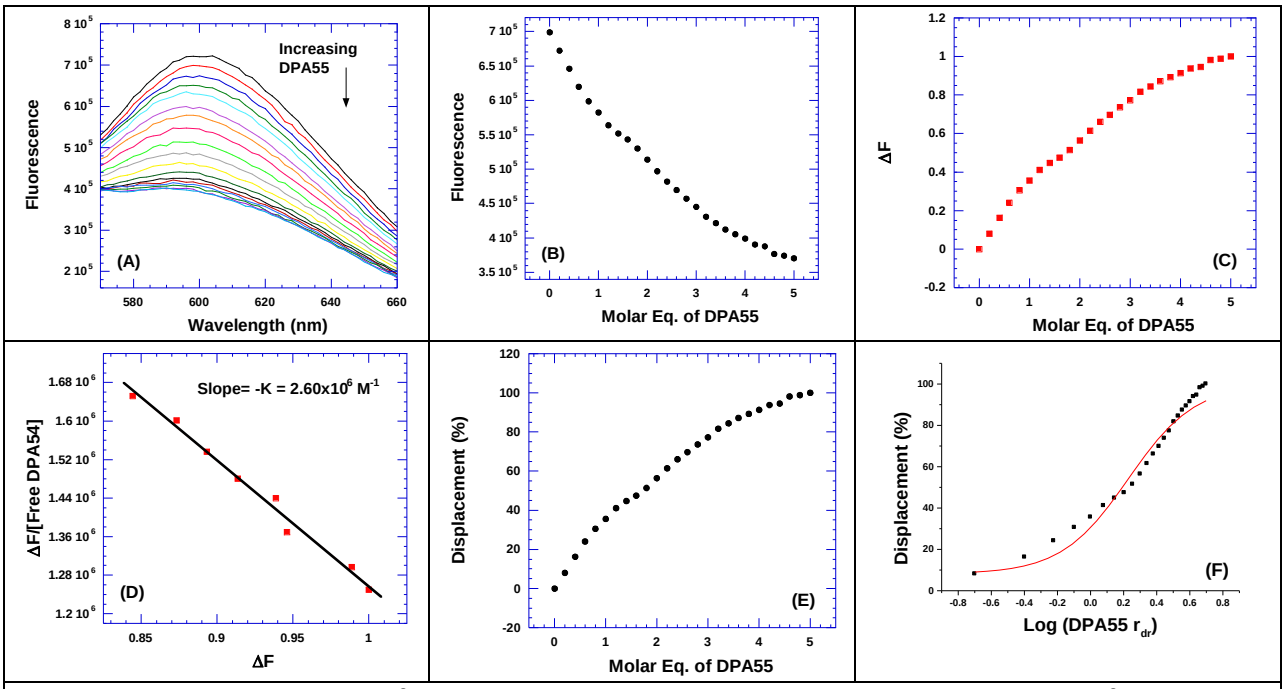

Figure S4.35. FID titration of **DPA55** with the **U3 bulge TAR RNA mutant**. Raw fluorescence emission spectra in the presence of increasing concentration of **DPA55** (A). The decrease of fluorescence intensity (at 610 nm) of the U3 bulge TAR RNA mutant/EtBr complex with increasing concentration of **DPA55** results in a saturating binding plot (B). The plot between normalized fluorescence intensity (at 610 nm) of the U3 bulge TAR RNA mutant-EtBr complex as a function of concentration of **DPA55** results in a saturating binding plot (C). The Scatchard plot analysis of **DPA55** with the U3 bulge TAR RNA mutant (D). The plot between normalized EtBr displacement (at 610 nm) of the U3 bulge TAR RNA mutant-EtBr complex as a function of concentration of **DPA55** (E). The plot for EtBr displacement (%) of the U3 bulge TAR RNA mutant-EtBr complex versus the log of the **DPA55** r_{dr}, the data shown with a sigmoidal fit, was used to determine the IC_{50} value (F). Buffer conditions: 100 mM KCl, 10 mM SC, 0.5 mM EDTA, pH 6.8. U3 bulge TAR RNA mutant = 200 nM/strand. [EtBr] = 5 µM.

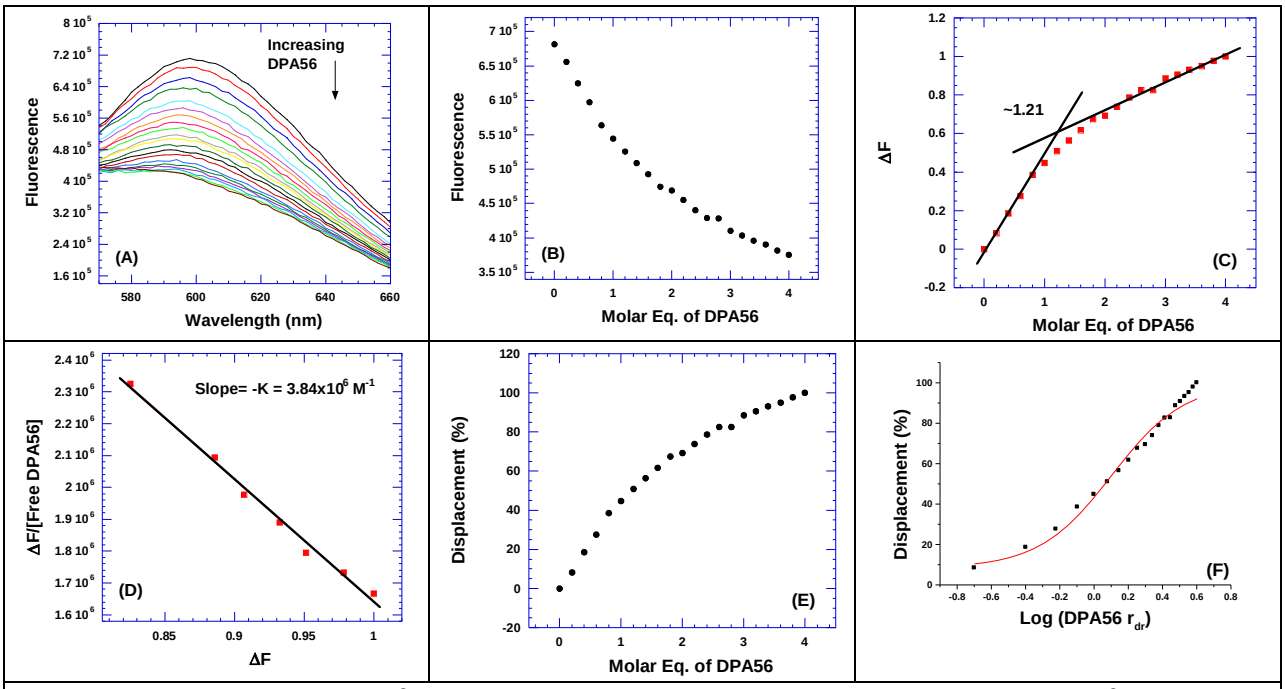

Figure S4.36. FID titration of **DPA56** with the **U3 bulge TAR RNA mutant**. Raw fluorescence emission spectra in the presence of increasing concentration of **DPA56** (A). The decrease of fluorescence intensity (at 610 nm) of the U3 bulge TAR RNA mutant/EtBr complex with increasing concentration of **DPA56** results in a saturating binding plot (B). The plot between normalized fluorescence intensity (at 610 nm) of the U3 bulge TAR RNA mutant-EtBr complex as a function of concentration of **DPA56** results in a saturating binding plot (C). The Scatchard plot analysis of **DPA56** with the U3 bulge TAR RNA mutant (D). The plot between normalized EtBr displacement (at 610 nm) of the U3 bulge TAR RNA mutant-EtBr complex as a function of concentration of **DPA56** (E). The plot for EtBr displacement (%) of the U3 bulge TAR RNA mutant-EtBr complex versus the log of the **DPA56** r_{dr}, the data shown with a sigmoidal fit, was used to determine the IC_{50} value (F). Buffer conditions: 100 mM KCl, 10 mM SC, 0.5 mM EDTA, pH 6.8. U3 bulge TAR RNA mutant = 200 nM/strand. [EtBr] = 5 µM.

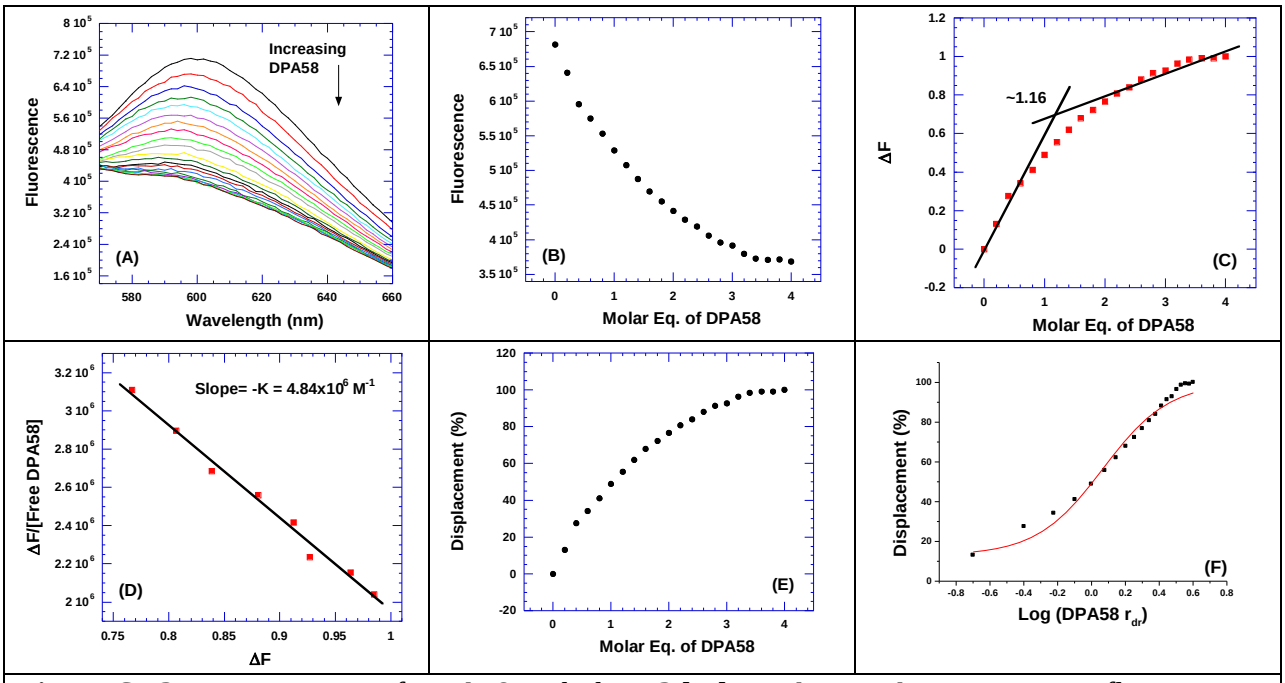

Figure S4.37. FID titration of **DPA58** with the **U3 bulge TAR RNA mutant**. Raw fluorescence emission spectra in the presence of increasing concentration of **DPA58** (A). The decrease of fluorescence intensity (at 610 nm) of the U3 bulge TAR RNA mutant/EtBr complex with increasing concentration of **DPA58** results in a saturating binding plot (B). The plot between normalized fluorescence intensity (at 610 nm) of the U3 bulge TAR RNA mutant-EtBr complex as a function of concentration of **DPA58** results in a saturating binding plot (C). The Scatchard plot analysis of **DPA58** with the U3 bulge TAR RNA mutant (D). The plot between normalized EtBr displacement (at 610 nm) of the U3 bulge TAR RNA mutant-EtBr complex as a function of concentration of **DPA58** (E). The plot for EtBr displacement (%) of the U3 bulge TAR RNA mutant-EtBr complex versus the log of the **DPA58** r_{dr}, the data shown with a sigmoidal fit, was used to determine the IC_{50} value (F). Buffer conditions: 100 mM KCl, 10 mM SC, 0.5 mM EDTA, pH 6.8. U3 bulge TAR RNA mutant = 200 nM/strand. [EtBr] = 5 µM.

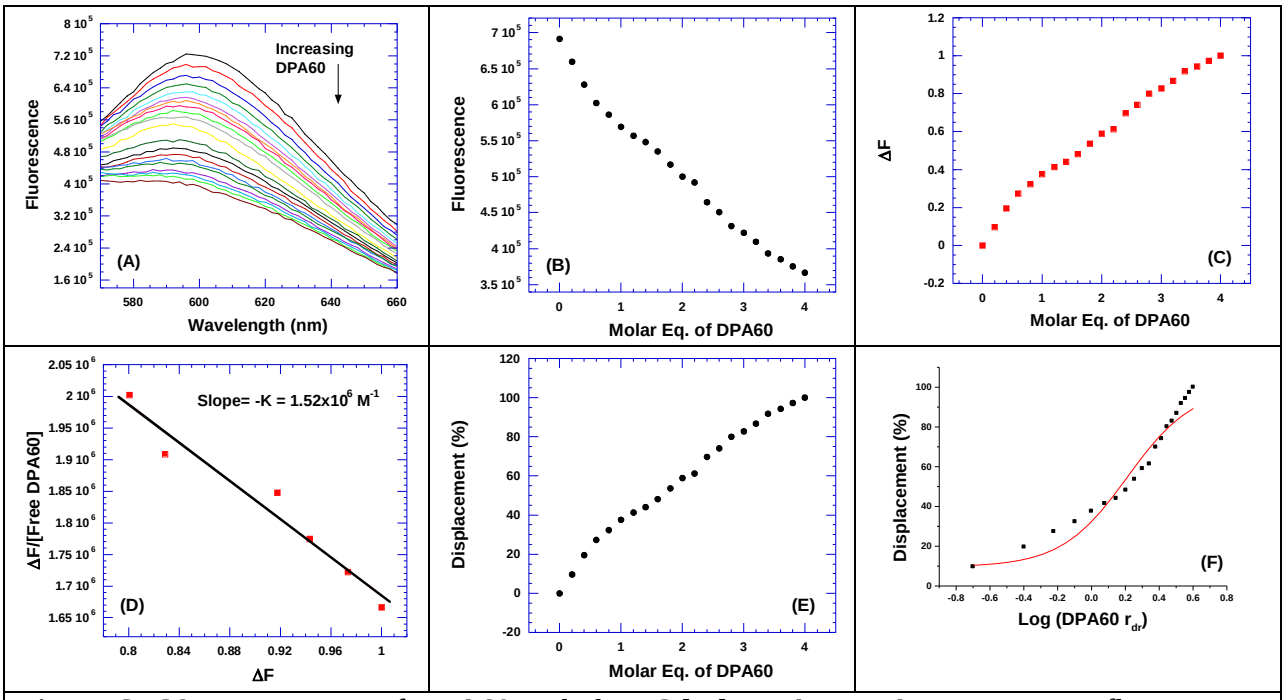

Figure S4.38. FID titration of **DPA60** with the **U3 bulge TAR RNA mutant**. Raw fluorescence emission spectra in the presence of increasing concentration of **DPA60** (A). The decrease of fluorescence intensity (at 610 nm) of the U3 bulge TAR RNA mutant/EtBr complex with increasing concentration of **DPA60** results in a saturating binding plot (B). The plot between normalized fluorescence intensity (at 610 nm) of the U3 bulge TAR RNA mutant-EtBr complex as a function of concentration of **DPA60** results in a saturating binding plot (C). The Scatchard plot analysis of **DPA60** with the U3 bulge TAR RNA mutant (D). The plot between normalized EtBr displacement (at 610 nm) of the U3 bulge TAR RNA mutant-EtBr complex as a function of concentration of **DPA60** (E). The plot for EtBr displacement (%) of the U3 bulge TAR RNA mutant-EtBr complex versus the log of the **DPA60** r_{dr}, the data shown with a sigmoidal fit, was used to determine the IC_{50} value (F). Buffer conditions: 100 mM KCl, 10 mM SC, 0.5 mM EDTA, pH 6.8. U3 bulge TAR RNA mutant = 200 nM/strand. [EtBr] = 5 µM.

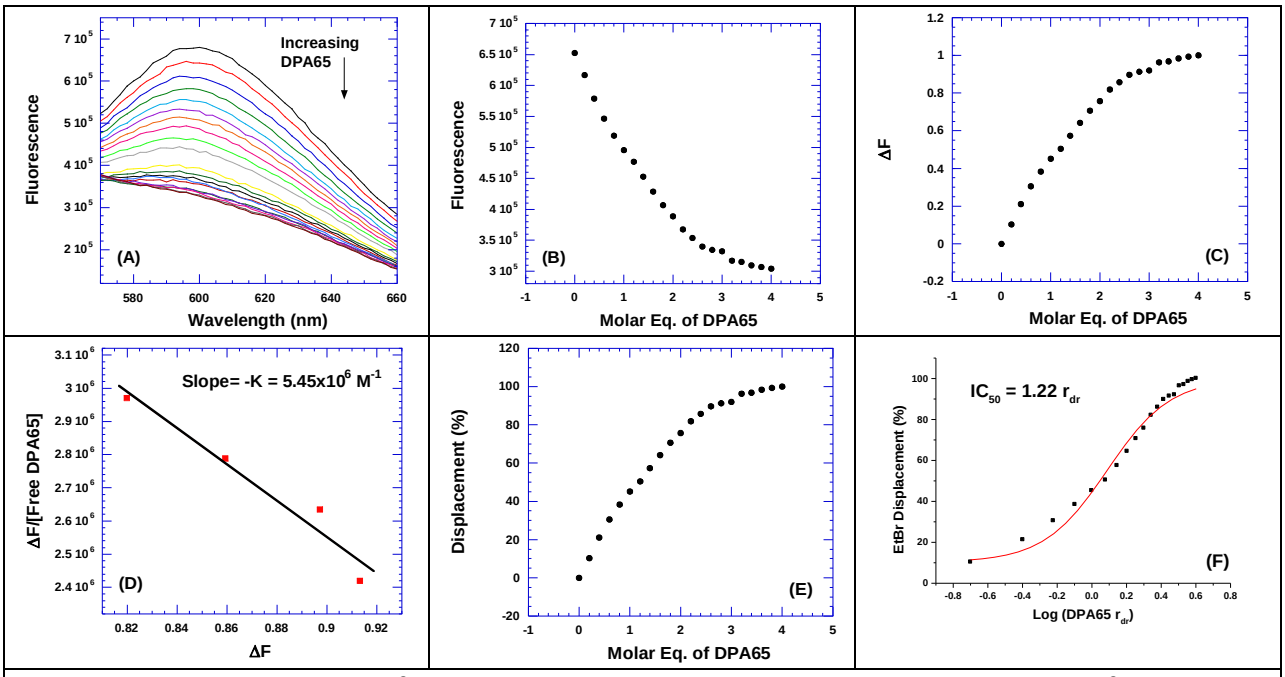

Figure S4.39. FID titration of **DPA65** with the **U3 bulge TAR RNA mutant**. Raw fluorescence emission spectra in the presence of increasing concentration of **DPA65** (A). The decrease of fluorescence intensity (at 610 nm) of the U3 bulge TAR RNA mutant/EtBr complex with increasing concentration of **DPA65** results in a saturating binding plot (B). The plot between normalized fluorescence intensity (at 610 nm) of the U3 bulge TAR RNA mutant-EtBr complex as a function of concentration of **DPA65** results in a saturating binding plot (C). The Scatchard plot analysis of **DPA65** with the U3 bulge TAR RNA mutant (D). The plot between normalized EtBr displacement (at 610 nm) of the U3 bulge TAR RNA mutant-EtBr complex as a function of concentration of **DPA65** (E). The plot for EtBr displacement (%) of the U3 bulge TAR RNA mutant-EtBr complex versus the log of the **DPA65** r_{dr}, the data shown with a sigmoidal fit, was used to determine the IC_{50} value (F). Buffer conditions: 100 mM KCl, 10 mM SC, 0.5 mM EDTA, pH 6.8. U3 bulge TAR RNA mutant = 200 nM/strand. [EtBr] = 5 µM.

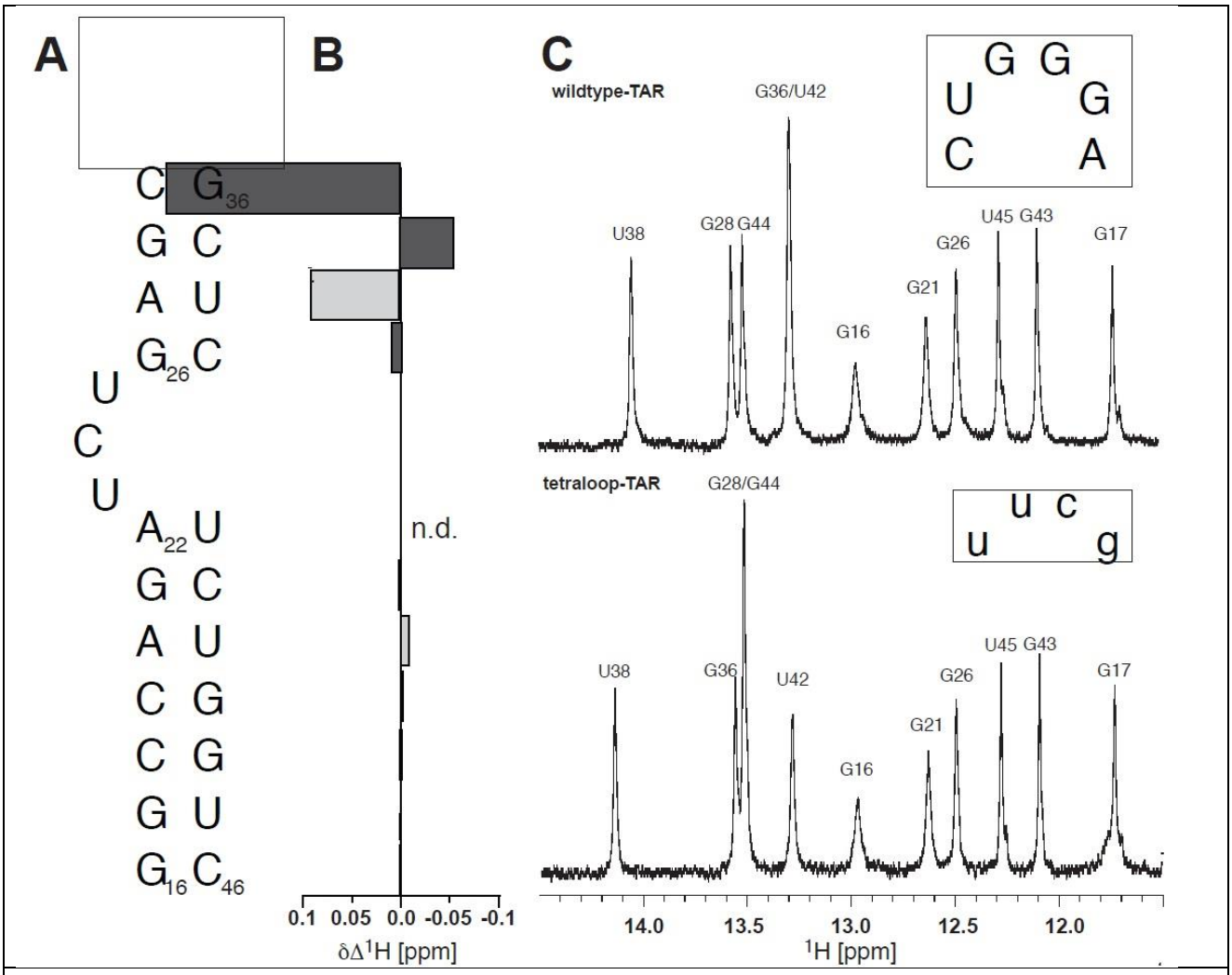

Figure S5.1 (A) Secondary structure (stems + bulge) of TAR variants used for NMR studies. (B) Chemical shift changes ($\Delta\delta = \delta_{tetra} - \delta_{wildtype}$ [ppm]) of GH1 (dark gray bars) and UH3 (light gray bars), respectively. Overlapped- or imino resonances broadened beyond detection are labeled n.d. (not determined) (C) Imino regions of 1D ^{1}H-jump-return echo experiments of wildtype- and tetraloop TAR. Data were collected on TAR variant samples containing ca. 0.25 mM RNA in 500 µl volume of NMR buffer. Spectra were recorded at 298K on a Bruker Avance III 850 MHz spectrometer.

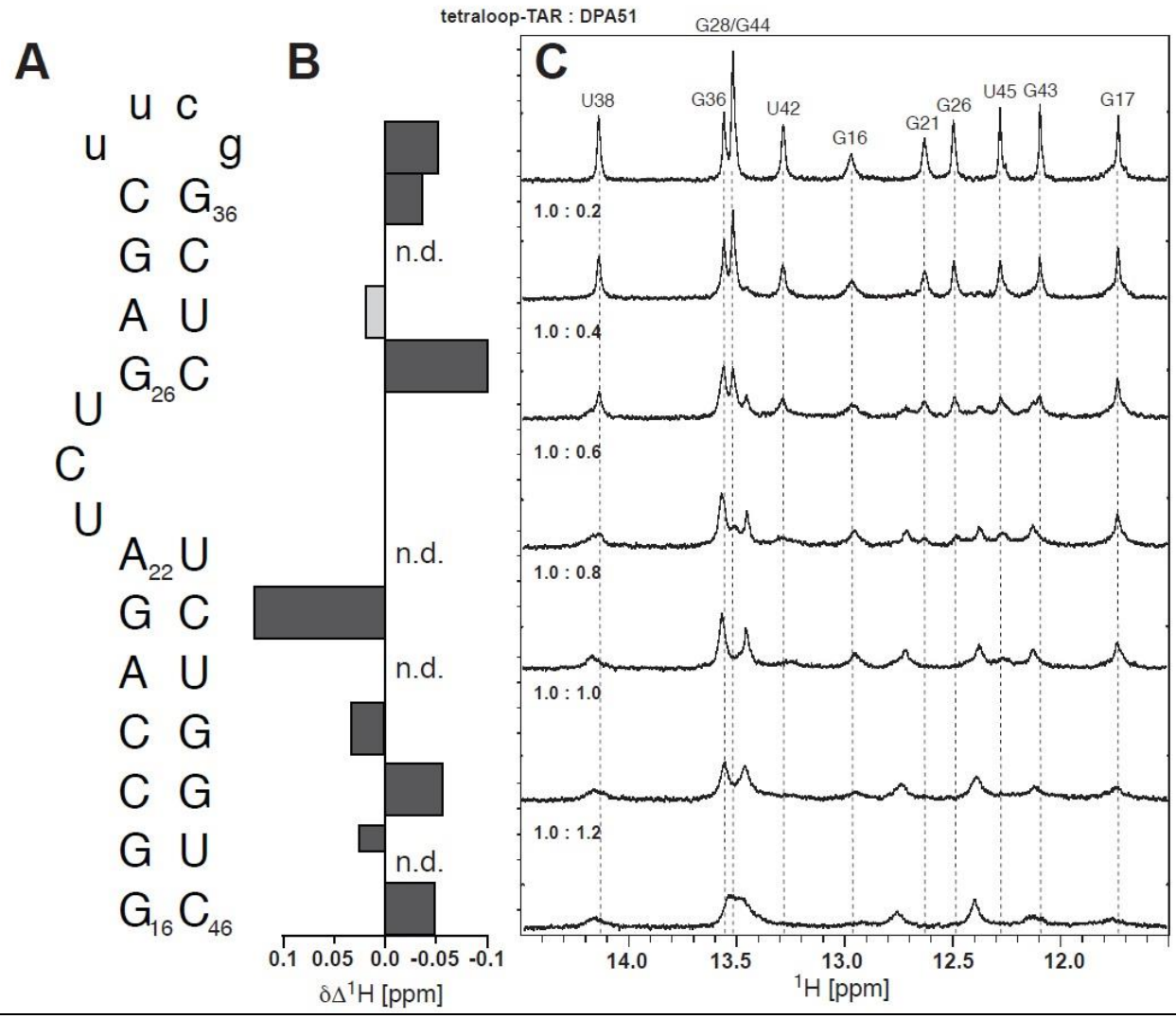

Figure S5.2. (A) Secondary structure of tetraloop TAR used for NMR studies. (B) Chemical shift changes ($\Delta\delta = \delta_{bound} - \delta_{free}$ [ppm]) of GH1 (dark gray bars) and UH3 (light gray bars), respectively, observed for the tetraloop TAR-**DPA51** complex. Overlapped- or imino resonances broadened beyond detection are labeled n.d. (not determined) (C) Imino regions of 1D ^{1}H-jump-return echo experiments of tetraloop TAR with increasing amounts of DPA51. Data were collected on a tetraloop TAR sample containing ca. 0.25 mM RNA in 500 µl volume of NMR buffer. Spectra were recorded at 298K on a Bruker Avance III 850 MHz spectrometer. Dashed black lines follow assigned imino proton resonances at various molar ratios of tetraloop TAR:**DPA51**.